NJC

Accepted Manuscript

ROYAL SOCIETY OF CHEMISTRY

www.rsc.org/njc

View Article Online
DOI: 10.1039/C4NJ02427C

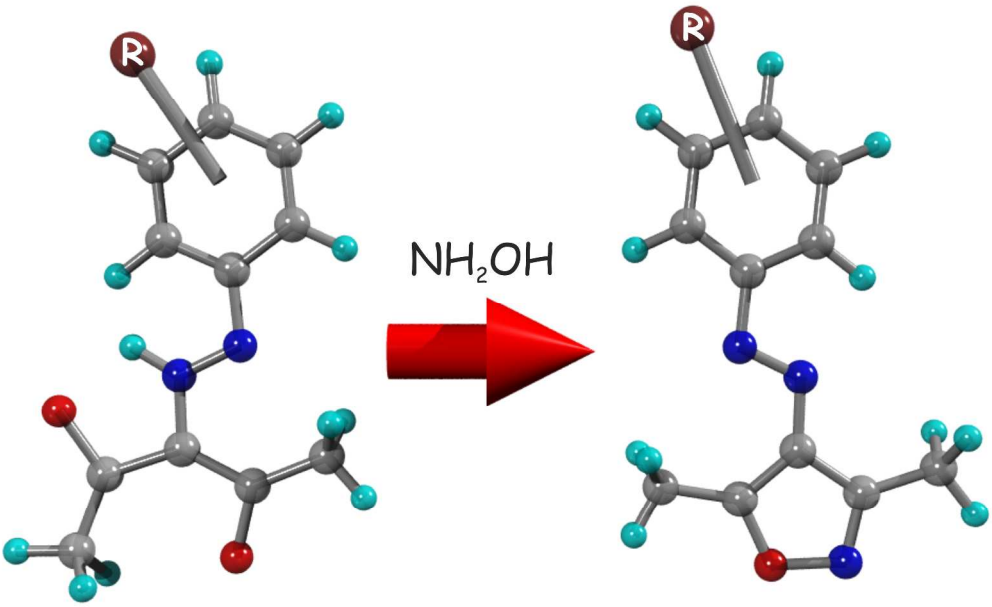

View Article Online
DOI: 10.1039/C4NJ02427C

New 3,4,5-Trisubstituted Isoxazoles Derivatives with potential biological properties

Carlos Bustos[a,*], Elies Molins[b], Juan-Guillermo Cárcamo[c], Marcelo N. Aguilar[c], Christian Sánchez[a], Ignacio Moreno-Villoslada[a], Hiroyuki Nishide[d], Angela Mesías-Salazar[a], Ximena Zarate[e], Eduardo Schott[f,*]

[a]*Instituto de Ciencias Químicas, Universidad Austral de Chile, Las Encinas 220, Campus Isla Teja, Valdivia, Chile.*

[b]*Institut de Ciència de Materials de Barcelona (ICMAB-CSIC), Campus de la Universitat Autònoma de Barcelona, 08193 Bellaterra, Spain.*

[c]*Instituto de Bioquímica y Microbiología, Universidad Austral de Chile, Campus Isla Teja, Valdivia, Chile.*

[d]*Department of Applied Chemistry, School of Science and Engineering, Waseda University, Tokyo 169-8555, Japan.*

[e]*Dirección de Postgrado e Investigacion, Universidad Autónoma de Chile, Av. Pedro de Valdivia 641 , Santiago, Chile.*

[f]*Laboratorio de Bionanotecnologia, Universidad Bernardo O'Higgins, General Gana 1702, Santiago, Chile.*

*email: maschotte@gmail.com, Phone/Fax: 56-2-24772243.

Keywords: Isoxazole, cytotoxic effect, synthesis, DFT, X-Ray

Abstract

Synthesis of (*E*)-3,5-dimethyl-4-(**R**-phenyldiazenyl)isoxazoles was carried out by reaction of β-diketohydrazones, of formula **R**-C_6H_4-NHN=$C(COCH_3)_2$ with hydroxilammonium chloride, being **R**= 4-$N(CH_3)_2$(**1**), 4-OH(**2**), 4-CH_3(**3**), 4-OCH_3(**4**), 4-H(**5**), 4-Cl(**6**) 4-Br(**7**), 4-CO2H(**8**), 4-$CO_2CH_2CH_3$(**9**), 4-$COCH_3$(10), 4-CN(**11**), 4-NO_2(**12**), 4-$CH_2CO_2CH_2CH_3$(**13**), 3-Cl(**14**), 2-OH(**15**),

View Article Online
DOI: 10.1039/C4NJ02427C

2-Cl(**16**), 2-NO_2(**17**), 2-CO_2H(**18**). All compounds were characterized by EA and spectroscopic methods. The crystalline structure of two compounds was solved by X-rays diffraction method. DFT and TDDFT computations were performed in order to characterize the molecular geometry and the molecular orbitals involved in the transitions. Besides, a biological activity study was performed to evaluate the toxicity of compounds towards human *promielocytic leukemia cell line*, HL-60, using MTT reduction method. The IC_{50} values are in a wide concentrations range, 86 - 755 μM. The isoxazoles (**3**) and (**6**) were the most cytotoxic. Expression analysis in HL-60 cells were carried out with compounds (**3**) and (**6**) by RT-PCR, in order to determine the effect on the expression levels of *m*RNA codifying for the genes Bcl-2, Bax and $p21^{WAF-1}$. The isoxazole (**3**) induced a decrease of the expression of Bcl-2, whereas the isoxazole (**6**) showed an opposite behaviour. However, these isoxazoles had no effect on *m*RNA levels of Bax. On the other hand, both isoxazoles increased the levels of $p21^{WAF-1}$. These results suggest that the cytotoxic activity of the isoxazole (**3**) would be the sum of effects triggered on promotion of apoptosis and cell cycle arrest, whereas for isoxazole (**6**) would be mainly through cycle cell arrest.

1. Introduction

The biological activity of substituted isoxazoles has made them a focus in medicinal chemistry in the last years[1], because they are potent selective agonists of human cloned dopamine D4 receptor[2], exhibit $GABA_A$ antagonist activity[3], as well as analgesic, antiinflamatory[4], antimicrobial and antifungal[5] activity. Also, they can inhibit COX-2 action[6,7] and present antinociceptive[8] and anticancer[9] activity.

Many synthetic methods have been used to obtain substituted isoxazoles[10] including reactions of hydroxylamine with 1,3-dicarbonyl compounds[11], α,β-unsaturated carbonyl compounds[12] and α,β-unsaturated nitriles[13]. The reaction of an oxime-derivative dianion with an ester[14] or amide[15,16] also

View Article Online
DOI: 10.1039/C4NJ02427C

yields isoxazoles. On the other hand, [3+2] cycloaddition reactions between alkynes and nitrile oxides have also been developed[17,18]. However, these methods often require strong bases, strong mineral acids or high temperatures or provide poor regioselectivity. Functionalizations of isoxazoles are also known[19]. Recently, three new methods involving a cascade reaction of nitrocompounds with oxetane-3-one[20] and gold/silver/copper-catalyzed[21,22] synthesis of di-substituted and tri-sustituted isoxazoles by cyclization of alkynyloxime ethers have been reported.

The method reported here allows obtaining isoxazoles under mild conditions by reaction of β-diketohydrazones with hydroxylammonium chloride. In this work, we present an extensive report on the synthesis and characterization of a new series of 3,4,5-trisubstituted isoxazoles using (3-(2-(4-**R**-phenyl)hydrazinylidene)pentane-2,4-diones[23-27] as precursors, where **R=** 4-$N(CH_3)_2$(**1**), 4-OH(**2**), 4-CH_3(**3**), 4-OCH_3(**4**), 4-H(**5**), 4-Cl(**6**) 4-Br(**7**), 4-CO2H(**8**), 4-$CO_2CH_2CH_3$(**9**), 4-$COCH_3$(10), 4-CN(**11**), 4-NO_2(**12**), 4-$CH_2CO_2CH_2CH_3$(**13**), 3-Cl(**14**), 2-OH(**15**), 2-Cl(**16**), 2-NO_2(**17**), 2-CO_2H(**18**). Crystals suitable for X-Ray diffraction were also obtained for two of the studied compounds. Furthermore, considering that numerous isoxazole derivatives have shown antineoplastic activity[28-32], a biological study was performed in order to evaluate the cytotoxic activity towards the *human promielocytic leukemia* cell *line*, HL-60. Moreover, using compounds with IC_{50} values lower than 100 μM, we performed RT-PCR experiments to determine the effect on the expression levels of *m*RNA that codifies for anti- and pro-apoptotic genes, Bcl-2 and Bax, and a gene involved in cell cycle progression, $p21^{WAF-1.}$

2. Result and discussion

2.1. Chemistry

View Article Online
DOI: 10.1039/C4NJ02427C

The chemical route for this reaction is shown in Scheme 1. The presence of the H-bond assisted by resonance on the carbonyl groups of the β-diketohydrazone, increases its electrophilic character providing a remarkable difference of the reactivity of both carbonyl groups. Thereby, controlling the reaction stoichiometry the condensation of one carbonyl group is allowed and the reaction with hydroxylammonium chloride yields only the mono-oxime as intermediate. Then, in acid media, the unreacted carbonyl group suffers an addition/displacement reaction to yield the corresponding isoxazoles. This synthetic approximation was used to improve the regioselectivity of the reaction of a series of (3-(2-(4-**R**-phenyl)hydrazinylidene)pentane-2,4-diones with NH_2OH•HCl, using 1:1 stoichiometric ratio. HOAc was used as catalyst in refluxing EtOH, 18 h. The reaction products, (*E*)-3,5-dimethyl-4-(**R**-phenyldiazenyl)isoxazoles (**1**)-(**18**), Scheme 1, are obtained with high yields (over 65%) and were recrystallized in mixtures EtOH/H_2O of variable composition. Compounds (**7**) and (**17**) yielded single crystals, suitable for X-ray diffraction studies. The crystallographic results are in concordance with the previously obtained structures, *vide infra*[23].

Scheme 1

View Article Online
DOI: 10.1039/C4NJ02427C

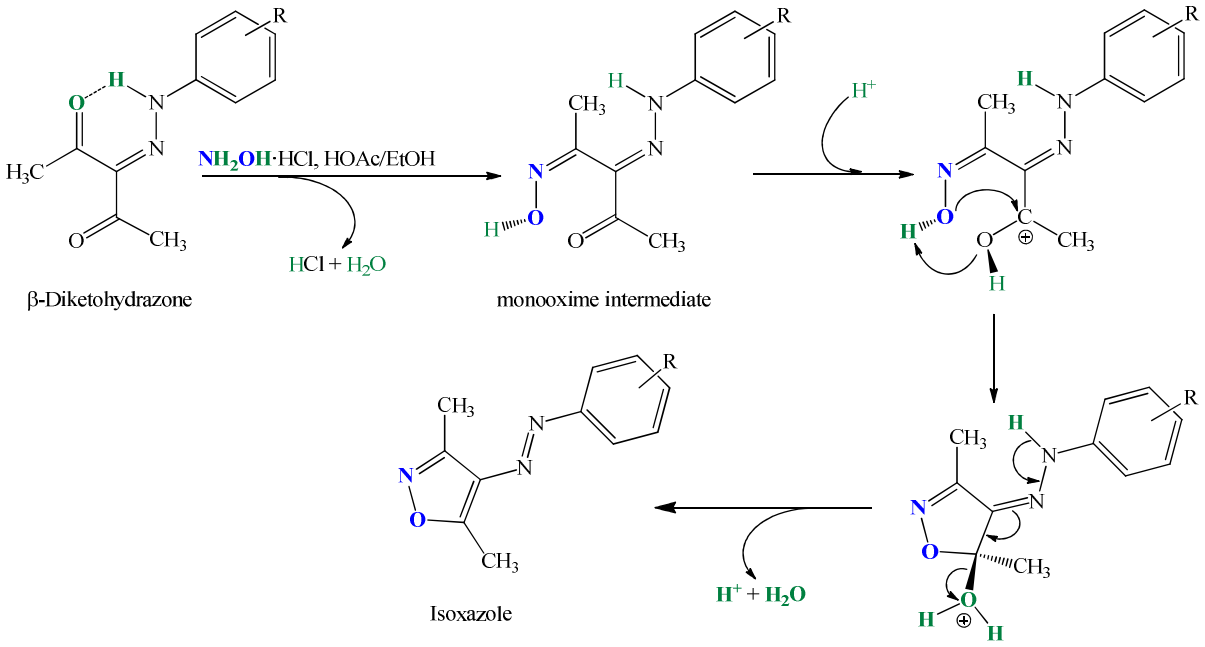

R= *4*-N(CH$_3$)$_2$ (**1**), *4*-OH (**2**), *4*-CH$_3$ (**3**), *4*-OCH$_3$ (**4**), *4*-H (**5**), *4*-Cl (**6**), *4*-Br (**7**), *4*-CO$_2$H (**8**), *4*-CO$_2$CH$_2$CH$_3$ (**9**), *4*-COCH$_3$ (**10**), *4*-CN (**11**), *4*-NO$_2$ (**12**), *4*-CH$_2$CO$_2$CH$_2$CH$_3$ (**13**), *3*-Cl (**14**), *2*-OH (**15**), *2*-Cl (**16**), *2*-NO$_2$ (**17**), *2*-CO$_2$H (**18**).

2.2. *Description of the structures*

Table 1 displays the selected bond distances, angles and torsion angles found for (**7a-7d**) and (**17**). Besides, Figures 1 and 2 show an ORTEP views of (**7b**) and (**17**), respectively, and the crystal data and refinement parameters of the structures are shown in Table 2. Both structures were compared with the structure of compound (**18**) previously described in the literature[23], whose geometrical parameters have been also incorporated in Table 1. Compound (**7**) crystallizes in the monoclinic system, space group P2$_1$/*n*, with cell parameters *a*= 13.5334(6) Å, *b*= 12.3004(8) Å, *c*= 28.098(2) Å, β= 102.177(6)° and Z= 16. The structure has been refined with final indices, [*I* >2*σ*(*I*)], *R1*= 0.0789, *wR2*= 0.1448 and *S*= 1.056, Table 2. On the other hand, compound (**17**) crystallizes in a monoclinic system, space group C2/*c*, with cells parameters *a*= 11.765(4) Å, *b*= 11.314(6) Å y *c*= 17.774(12) Å, β= 95.75(4)° and Z= 4 and it has final indices, [*I* >2*σ*(*I*)], *R1*= 0.0597, *wR2*= 0.1492 and *S*= 1.026, Table 2. The asymmetric unit of (**7**) contains four molecules of

View Article Online
DOI: 10.1039/C4NJ02427C

isoxazole, (**7a**)-(**7d**), where (**7a**) has a 50 % of disorder on the fragment N(1)-N(2)-C(6) affecting also the bond distances and angles located in their surroundings, Table 1. In (**7a**) the N(1)-N(2) and N(2)-C(6) distance values indicate that there is a certain sp^2 distortion in this fragment, which is corroborated by a significant change in the respective bond angle N(1)-N(2)-C(6), Table 1. However, the rest of the molecules, (**7b**)-(**7d**) and (**17**), exhibit geometrical parameters similar to those found in compound (**18**)[23]. Both structures contain a C(1)-N(1)-N(2)-C(6) moiety with *E* configuration around the -N=N- bridge, with an important degree of π-delocalization, *vide infra*. The torsion angles involved in this molecular fragment indicate that the molecules have geometry basically planar, Table 1. Finally, there are no conventional intermolecular hydrogen bonds and the entire supramolecular structure is constructed only by weak interactions. The crystallographic information of the structures described in this article has been included as supplementary material.

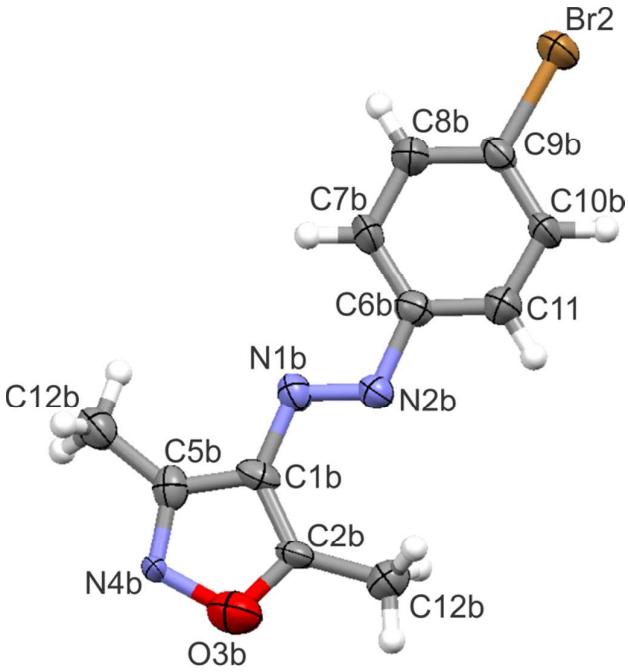

Figure 1. ORTEP view of the molecule (**7b**) of the compound (**7**) with a probability level of 50%.

View Article Online
DOI: 10.1039/C4NJ02427C

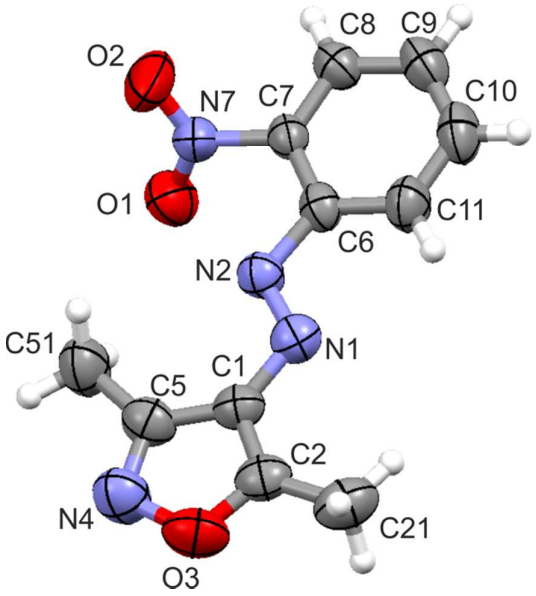

Figure 2. ORTEP view of compound (**17**) with a probability level of 50%

Table 1. Selected bond lengths (Å), bond angles (º) and torsion angles (º) in the asymmetric unit of the four molecules of (**7**) and (**17**) compared with the structural data of (**18**)[23] obtained from literature, where (*) shows the disorder found in (**7a**).

Bond/Angle	7a	7b	7c	7d	17	18
C(2)-C(1)	1.372(8)	1.399(7)	1.424(6)	1.385(7)	1.351(4)	1.347(3)
C(1)-N(1)	1.411(10) *1.500(14)	1.413(6)	1.424(6)	1.414(6)	1.385(4)	1.403(3)
C(1)-C(5)	1.413(8)	1.368(7)	1.370(7)	1.399(7)	1.429(4)	1.418(4)
C(2)-O(3)	1.330(7)	1.320(6)	1.326(6)	1.338(6)	1.339(4)	1.352(3)
C(5)-N(4)	1.321(7)	1.330(6)	1.317(6)	1.314(6)	1.300(4)	1.301(3)

View Article Online
DOI: 10.1039/C4NJ02427C

N(2) -C(6)	1.437(14) *1.63(3)	1.432(6)	1.427(6)	1.430(7)	1.423(4)	1.431(3)
N(1)-N(2)	1.249(13) *1.253(16)	1.258(6)	1.259(6)	1.264(6)	1.257(3)	1.254(3)
O(3)-N(4)	1.450(7)	1.446(6)	1.423(6)	1.435(7)	1.426(4)	1.424(3)
C(2)-C(1)-N(1)	114.2(7)	130.2(5)	131.9(5)	120.6(5)	122.5(3)	121.1(2)
C(2)-C(1)-C(5)	105.7(5)	106.0(5)	106.2(4)	105.9(4)	104.8(3)	105.8(2)
N(1)-C(1)-C(5)	140.0(7) *105.4(7)	123.6(5)	121.8(5)	133.4(5)	132.7(3)	133.1(2)
O(3)-C(2)-C(1)	110.3(6)	109.3(5)	109.4(5)	109.3(5)	109.9(3)	109.4(2)
N(4)-C(5)-C(1)	110.1(6)	111.1(5)	109.3(5)	110.3(5)	111.2(3)	110.6(2)
N(2)-N(1)-C(1)	112.3(10) 99.4(11)	114.9(5)	114.2(5)	113.0(5)	114.0(3)	113.2(2)
N(1)-N(2)-C(6)	109.4(12) *92.9(15)	114.2(5)	115.0(4)	112.9(5)	113.7(3)	113.0(2)
C(7)-C(6)-N(2)	103.0(13) *147(2)	124.9(5)	124.2(5)	114.6(5)	117.3(3)	119.2(2)
C(7)-C(6)-N(2)-N(1)	173(3)	4.9(8)	3.4(8)	171.1(5)	176.5(3)	153.8(2)

View Article Online
DOI: 10.1039/C4NJ02427C

C(6)-N(2)-N(1)-C(1)	178(3)	179.5(5)	-179.1(5)	178.7(4)	-178.2(3)	176.6(2)
N(2)-N(1)-C(1)-C(5)	-10(2)	179.0(5)	-179.8(5)	-7.6(9)	5.7(5)	7.3(4)
N(2)-N(1)-C(1)-C(2)	174.6(9)	-6.7(9)	4.4(9)	174.5(5)	-176.7(3)	-173.1(2)

2.3. Pauling's bond orders studies

In order to know the π-delocalization degree of the fragment C(2)-C(1)-N(1)-N(2)-C(6) in compounds (**7b**)-(**7d**), (**17**) and (**18**), the Pauling's bond orders, *n*, and the conjugation parameters, η, were calculated using the structural data shown in the Table 1. The bond orders found for n_1 (C(2)-C(1)), n_2 (C(1)-N(1)), n_3 (N(1)-N(2)), and n_4 (N(2)-C(6)) have intermediates values between ideal orders 1 and 2 for single and double bonds, respectively; which is in concordance with the presence of a delocalized system, Table 2.

Table 2. Pauling's bond orders, *n*, and π-delocalization parameters, η, of compounds (**7b**)-(**7d**), (**17**) and (**18**) calculated for the fragments C(2)-C(1)-N(1)-N(2)-C(6). (**7a**) was not included due to disorder.

Compound	n_1	n_2	n_3	n_4	$\%\eta_{1,2}$	$\%\eta_{2,3}$	$\%\eta_{3,4}$
(**7b**)	1.4504	1.2000	1.7240	1.1283	38	76	20

View Article Online
DOI: 10.1039/C4NJ02427C

(**7c**)	1.3368	1.1581	1.7184	1.1468	41	78	21
(7d)	1.5181	1.1964	1.6906	1.1356	34	75	22
(17)	1.6961	1.3152	1.7297	1.1619	31	71	22
(18)	1.7184	1.2418	1.7467	1.1319	26	75	19

The n_1 and n_3 values show a decrease of the double bond character of the C(2)-C(1) and N(1)-N(2). However n_1 value shows that the C(2)-C(1) bond has a higher decrease of double bond character respect to the bond N(1)-N(2). On the contrary, an increase of both n_2 and n_4 values respect to the formal single bonds C(1)-N(1) and N(2)-C(6) were found. These observations indicate an intense π-delocalization on the complete fragment C(2)-C(1)-N(1)-N(2)-C(6). The π-delocalization is corroborated by the η values found for sub fragments C(2)-C(1)-N(1), C(1)-N(1)-N(2), and N(1)-N(2)-C(6), whose π-delocalization values $\%\eta_{1,2}$, $\%\eta_{1,2}$, and $\%\eta_{3,4}$ takes values in the ranges of 26-41 %, 71-78 %, and 19-22 %, respectively, Table 2. The increase of $\%\eta_{1,2}$ values respect to $\%\eta_{3,4}$ indicate that the π-delocalization is more intense in the sub fragment C(1)-N(1)-N(2) which is part of the isoxazole ring. These observed features are in concordance with the structural data discussed above and with the basically planar geometry for the fragment C(2)-C(1)-N(1)-N(2)-C(6) deduced from the torsion angles shown in Table 1.

2.4. Spectroscopic studies

The UV-visible absorption spectra of compounds (**1**)-(**18**) were registered in ethanol solutions and exhibit one main $\pi^* \leftarrow \pi$ absorption band placed in the ranges of 392-315 nm. This transition is very intense, $log\varepsilon$:4.36-4.18, probably due to a $\pi^* \leftarrow \pi$ absorption that emerge from the π-delocalized

View Article Online
DOI: 10.1039/C4NJ02427C

-C=C-N=N-C- chromophore present in each isoxazole molecule, see Scheme 1 and TDDFT calculations. This transition does not show correlation with the Hammett equation, $log\lambda$ vs σ_p (data not shown). Other intense $\pi^* \leftarrow \pi$ absorption bands located at higher energies have been attributed to the internal absorption of the phenyl rings.

The IR spectra of compounds (**1**)-(**18**), recorded in solid state, exhibit three typical stretching absorption between 1595-1619, 1600-1490 and 1416-1403 cm^{-1}, attributed to the ν(C=N) and/or ν(N=N), ν(C=C) and ν(N-O) chromophores, respectively. Moreover, the spectra also show the weak absorptions corresponding to the aromatic and aliphatic stretching modes, ν(C-H), around 3000 cm^{-1}, respectively and the characteristic stretching absorptions attributed to the substituent groups.

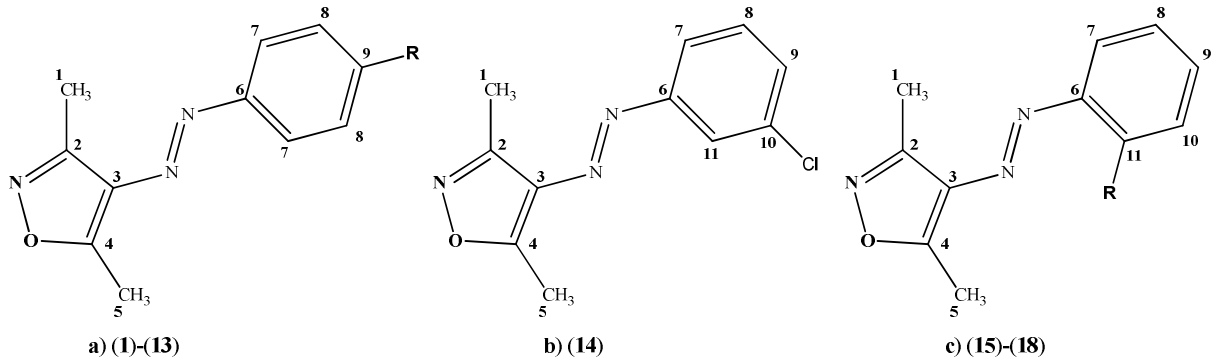

Figure 3. Labelling of atoms for the assignment of ^1H and ^{13}C NMR signals in the spectra.

The outstanding features of the ^1H NMR spectra of (**1**)-(**18**) are two singlets placed at 2.42-2.57 and 2.70-2.80 ppm ranges attributed to the protons linked to the carbon atoms C_1 and C_5, respectively, Figure 3. Besides, these compounds exhibit the resonances attributed to the aromatic protons in the 6.67-8.14 ppm range. The corresponding signals due to the substituent groups are also observed.

View Article Online
DOI: 10.1039/C4NJ02427C

On the other hand, the ^{13}C NMR spectra show all resonances corresponding to the isoxazole carbon atoms, the phenyl rings and the resonances that emerge from each substituent group. An important aspect of these spectra is the almost invariable chemical shifts of the carbon atoms C_1, C_2, C_3, C_4 and C_5, whose positions are in the narrow ranges of 12.29-11.46, 154.75-152.84, 133.50-131.45, 171.90-166.49 and 11.98-11.98 ppm, respectively.

Additionally, the HMBC spectra were recorded in order to assign the carbon and hydrogen resonances of the isoxazole ring. As an example, Figure 4 shows the HMBC spectrum of compound (**2**) that show the common interaction pattern present in the isoxazole rings. In fact, the protons of the $^{1}CH_3$- group interact with C_2 and C_3, while protons of the $^{5}CH_3$- group interact with carbon C_4 and also C_3. In this figure it is possible to observe also the H-C interactions attributed to the phenyl ring.

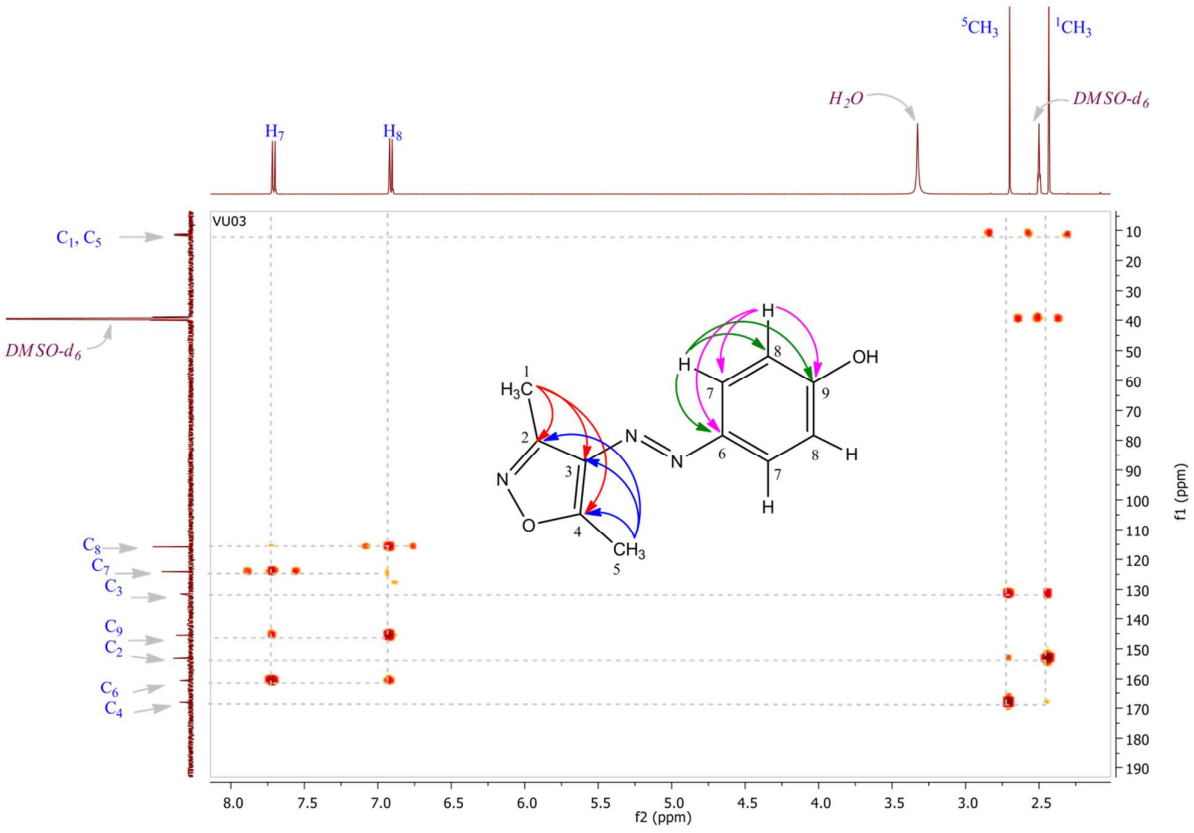

Figure 4. HMBC spectrum of compound (**2**) in *DMSO-d_6* showing the H-C interactions.

View Article Online
DOI: 10.1039/C4NJ02427C

2.5. Computational study

To get further in the characterization of compounds (**1**)-(**18**), we carried out theoretical calculations in order to give a better explanation to some previously mentioned facts. It is possible to observe that in the optimized molecular structures, see Table S1, the bond lengths and angles are unaffected by the change of the -**R** substituent. The substituents were changed from electron-withdrawing to electron-donor groups in the different positions of the phenyl rings. The observed changes are about 0.03 Å and 10°. The bond lengths that show more variation correspond to those bonds involved in the substituted phenyl rings.

In order to assure that each optimized structure corresponds to energy minimum, vibrational frequencies were calculated. Only positive frequencies were observed with a very good concordance between the experimental and the theoretical IR spectra, see Figure 5 for compound (**2**). In the characterization of these vibrational frequencies we found that the signals located in the range 1595-1619 cm^{-1} of the experimental IR spectra, correspond to the chromophores -C=N- and -N=N-, see Table S2.

View Article Online
DOI: 10.1039/C4NJ02427C

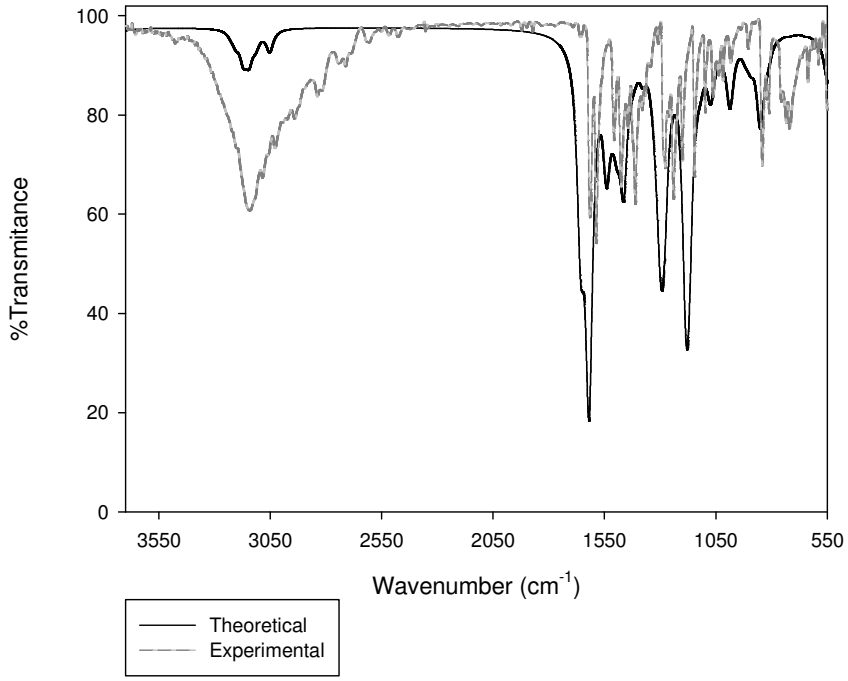

Figure 5. Experimental and theoretical plot of the obtained IR spectra for (**2**).

To perform a characterization of the UV-vis spectra of (**1**)-(**18**) TD-DFT computations were performed. All the calculated transitions are depicted in the supplementary information, Table S3, and a superimposition of the UV-VIS spectra of (**2**) and the calculated transition is shown in Figure 6. These computations indicate that the transition, located in the range 313-393 nm, correspond to the transition between HOMO-LUMO. These two involved orbitals are delocalized over the whole chain of each compound (see Supplementary Information). The absence of Hammett correlation could be explained considering the level of localization and the composition of these molecular orbitals, which does not depend on the nature of the substituent, placed on the azo phenyl group of compounds (**1**)-(**18**).

View Article Online
DOI: 10.1039/C4NJ02427C

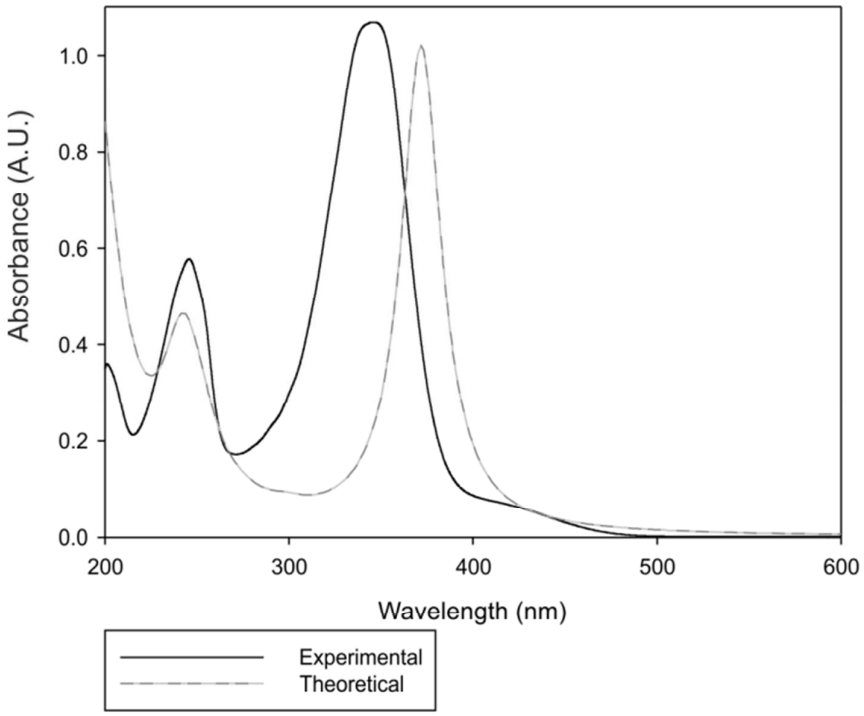

Figure 6. Experimental and theoretical plot of the obtained UV-vis spectra for compound (**2**).

2.6. Biological activity studies

2.6.1. ***Cytotoxic effect of isoxazoles***: Compounds (**1**)-(**18**) were subjected of *in vitro* biological studies by incorporating them to cultures of leukemia HL-60 cells. The cytotoxic effect was measured after exposure of the cells to the isoxazoles for 24 h, and was expressed as the relative change on the cell viability compared to the control sample (untreated cells). The IC_{50} values were obtained from dose-response curves and they fall in a wide range of concentrations, see Table 3. Isoxazoles (**3**) and (**6**) were the most active, with IC_{50} values of 95.4 and 85.6 μM, respectively. Interestingly both compounds are functionalized in the same position with substituents of similar size[33]. Both mentioned compounds which showed the highest cytotoxic activity toward HL-60 cells were subject of additional biological studies.

View Article Online
DOI: 10.1039/C4NJ02427C

Table 3. In vitro activity, IC_{50} values, of the isoxazoles toward HL-60 cells

Isoxazole	Substituent (R)	IC_{50} (μM)
(**1**)	*p*-$N(CH_3)_2$	285.0
(**2**)	*p*-OH	146.1
(**3**)	*p*-CH_3	95.4
(**4**)	*p*-OCH_3	153.6
(**5**)	*p*-H	151.4
(**6**)	*p*-Cl	85.6
(**7**)	*p*-Br	340.7
(**8**)	*p*-CO_2H	216.8
(**9**)	*p*-CH_2CO_2H	452.9
(**10**)	*p*-$COCH_3$	109.9
(**11**)	*p*-CN	165.5
(**12**)	*p*-NO_2	223.8
(**13**)	*p*-$CO_2CH_2CH_3$	192.1
(**14**)	*m*-Cl	754.9
(**15**)	*o*-OH	516.3
(**16**)	*o*-Cl	129.5
(**18**)	*o*-CO_2H	103.6
(**19**)	*o*-NO_2	102.9

2.6.2. ***Effect of the isoxazoles on expression of Bcl-2, Bax and p21^{WAF-1}***: Due to the interesting cytotoxic activity of (**3**) and (**6**) on HL-60 cells, we also explored their effect on the expression genes involved in apoptosis and cell cycle progression. Apoptosis is an active process of cell death that occurs in response to a variety of agents including ionizing radiation or anticancer chemotherapeutic drugs[34]. This implicates the balanced transcriptional control of anti-apoptotic and pro-apoptotic genes, such as Bax and Bcl-2. We have also included in this study a gene associated

View Article Online
DOI: 10.1039/C4NJ02427C

with the inhibition of the proliferation, $p21^{WAF-1}$. It is now well established that cyclins play a positive role in promoting cell cycle transitions *via* their ability to associate and activate their cognate cyclin dependent kinases (Cdks)[35-37]. Cdk2 associates with cyclins A, D and E has been implicated in the control of the G1 to S phase transition in mammals[35-37]. The protein $p21^{WAF1}$ is a potent, tight-binding inhibitor of Cdks and can inhibit the phosphorylation of Rb by cyclins complexes A-Cdk2, E-Cdk2, D1-Cdk4 and D2-Cdk4[38,39]. Thus, an increase of expression of $p21^{WAF-1}$ plays an important role in stopping of the cell cycle.

In order to determine the expression of Bax and Bcl-2 on the *m*RNA level, we performed a semi-quantitative duplex RT-PCR. Treatment of HL-60 cells with (**3**) at concentrations of IC_{50}, 95.4 µM, during 24 h, induces an important decrease on the expression of Bcl-2 to around 12 % relative to the control ($P< 0.05$), Figures 7A (lane 4) and 7D. Meanwhile, treatment with (**6**) at concentrations of IC_{50}, 85.6 µM during 24 h, increased the expression of Bcl-2 to 203% relative to the control, Figures 7A (lane 3) and 7D. Besides, under these experimental conditions, both (**3**) and (**6**) have no effect on *m*RNA levels of Bax, Figures 7B (lanes 4 and 3) and 7E, respectively. On the other hand, we found that (**3**) and (**6**) increased the levels of $p21^{WAF-1}$ *m*RNA expression to 340% and 365% relative to the control, respectively, Figures 7C (lanes 4 and 3) and 7F. The increase on the $p21^{WAF-1}$ *m*RNA expression indicates that the isoxazoles (**3**) and (**6**) would induce the arrest of cell cycle on the HL-60 cells. Thus, taken together the results suggest that the cytotoxic effect of (**3**) would be the sum of a decrease in Bcl-2, an anti-apoptotic protein, hence promoting the apoptosis, and by arrest of cell cycle through the increase of $p21^{WAF-1}$. Meanwhile the cytotoxic ability of (**6**) would be directed mainly by inhibition of the cell cycle through the increase of $p21^{WAF-1}$.

View Article Online
DOI: 10.1039/C4NJ02427C

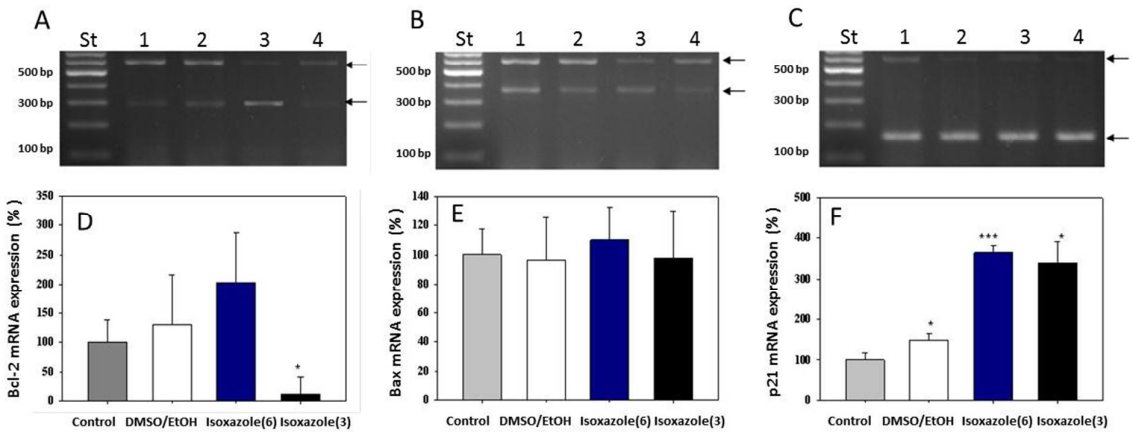

Figure 7. Effect of the (**3**) and (**6**) on *m*RNA expression levels of Bcl-2 (A and D), Bax (B and E) and p21^{WAF-1} (C and F) in HL-60 cells examined by semiquantitive duplex RT-PCR. PCR products were separated using 1.5% agarose gel electrophoresis, the arrows indicate the PCR products for GAPDH (600 bp), Bcl-2 (293 bp), Bax (332 bp) and p21^{WAF-1} (156 bp). Lane 1, untreated control; line 2, vehicle control; lane 3, treatment with 86 µM isoxazole (**6**); lane 4, treatment with 95 µM isoxazole (**3**). The PCR products were quantified relative to the internal standard GAPDH (D, E and F). The results are shown as mean ± standard deviations (SD) and correspond to the percentage change compared to the control sample assigned as 100%. Differences with *P* values of < 0.05 (*) or *P* values of < 0.01 (***) were considered significant.

3. Conclusions

A one-pot synthesis of a family of new 3,4,5-trisubstituted isoxazoles has been done with good yields, by treatment of β-diketohydrazones of the type (3-(2-(4-***R***-phenyl)hydrazinylidene)pentane-2,4-dione, with hydroxylammonium chloride in ethanol and acetic acid as catalyst. All compounds were characterized using elemental analysis and spectroscopic methods, (UV-vis, IR, ^{1}H NMR, ^{13}C NMR, and HMBC). The crystalline and molecular structure of (*E*)-3,5-dimethyl-4-((4-bromophenyl)diazenyl)isoxazole (**7**) and (*E*)-3,5-dimethyl-4-((2-nitrophenyl)diazenyl)isoxazole

View Article Online
DOI: 10.1039/C4NJ02427C

(**17**) were determined by X-ray diffraction methods. From the Pauling bond order, which were calculated from the crystallographic structure, it was possible to corroborate the delocalization of the system. The analytical, spectroscopic and structural data are in concordance with the proposed structures.

On the other hand, the cytotoxic activity of the most biologically active compounds was evaluated on *human promyelocytic leukemia cells*, HL-60. Compounds (**3**), (*E*)-3,5-dimethyl-4-(p-tolyldiazenyl)isoxazole, and (**6**), (*E*)-4-((4-chlorophenyl)diazenyl)-3,5-dimethylisoxazole, are the compounds that exhibit significant cytotoxic activity, with IC_{50} values below 100 μM and thus they would emerge as new potential molecules for further antineoplasic studies. In this context, the effect of both compounds on the expression of genes involved in apoptosis and in the cell cycle control has been evaluated. Compound (**3**) has an apoptotic effect, since the level of Bcl-2 *m*RNA decreases to approximately 12%. Importantly, both isoxazoles have an effect on the expression of $p21^{WAF-1}$, with an increase over 340% of the *m*RNA levels, suggesting a substantial anti-proliferative activity.

4. Experimental

4.1 Chemicals

Substitutes anilines, *R*-C_6H_4-NH_2 (*R*= 4-$N(CH_3)_2$ (**1**), 4-OH (**2**), 4-CH_3 (**3**), 4-OCH_3 (**4**), 4-H(**5**), 4-Cl (**6**) 4-Br (**7**), 4-CO_2H (**8**), 4-$CO_2CH_2CH_3$ (**9**), 4-$COCH_3$ (**10**), 4-CN (**11**), 4-NO_2 (**12**), 4-$CH_2CO_2CH_2CH_3$ (**13**), 3-Cl (**14**), 2-OH (**15**), 2-Cl (**16**), 2-NO_2 (**17**), 2-CO_2H (**18**)), acetylacetone, sodium nitrite, acetic acid, hydrochloric acid, sodium hydroxide and hydroxylammonium chloride were procured from Sigma-Aldrich Corporation and solvents, methanol, ethanol, diethylether, acetone $CDCl_3$, and *DMSO-*d_6, from the usual commercial sources, Merck, Fisher and T. J. Baker

View Article Online
DOI: 10.1039/C4NJ02427C

providers. All β-diketohydrazone precursors, *R*-C_6H_4-NHN=C($COCH_3$)$_2$ (*R*= *4*-N(CH_3)$_2$ (**1**), *4*-OH (**2**), *4*-CH_3 (**3**), *4*-OCH_3(**4**), *4*-H (**5**), *4*-Cl (**6**) *4*-Br (**7**), *4*-CO_2H (**8**), *4*-$CO_2CH_2CH_3$, (**9**), *4*-$COCH_3$ (**10**), *4*-CN (**11**), *4*-NO_2 (**12**), *4*-$CH_2CO_2CH_2CH_3$ (**13**), 3-Cl (**14**), 2-OH (**15**), 2-Cl (**16**), 2-NO_2 (**17**), 2-CO_2H (**18**)} were obtained using the method recommended in literature[24-27] and the structures were checked by IR spectroscopy and, in some cases, by NMR spectroscopy.

4.2 Physical measurements

Uncorrected melting points, MP, were determined on digital STUARD, SMP10 apparatus. Elemental analysis, EA; were obtained from a FISONS, EA 1118 microanalyses using sulfanilamide as standard. UV-Vis spectra were recorded in the 1100-200 nm range, in quartz cells with 10 mm length pass, using a Perkin Elmer, Lambda 35 spectrophotometer, and concentrated solutions, ~1.0×10^{-3} mole/L, of each compound, diluting around ~1.0×10^{-5} mole/L. The infrared spectra, IR, were obtained in solid state on an ATR *Jasco*, PRO450-S, mounted on a *Jasco*, FT/IR-4200 equipment. Depending of the solubility of compounds, ^{1}H NMR, ^{13}C NMR and HMBC spectra were recorded by the standard methods in *$CDCl_3$* or *DMSO-d_6* solutions, using 5 mm i.d. glass tubes and the internal solvent signals as reference, in two different equipments i) JOEL, JNM-Lambda500 spectrophotometer and ii) a Bruker, Avance AM 400 spectrophotometer. Assignment of ^{1}H and ^{13}C NMR signals was realized in accord with Figure 3.

4.3 Data collection

Single crystal X-ray diffraction data set for (**17**) was collected at room temperature up to a max 2θ of *ca.* 52º on an Enraf-Nonius CAD4 diffractometer using monochromatic MoKα radiation, λ= 0.71069 Å and ω-2ϑ scan mode. For (**7**), the experiment was done on a Bruker-CCD Smart 1 K

View Article Online
DOI: 10.1039/C4NJ02427C

diffractometer using also MoKα radiation. Crystal data and structure refinement are shown in Table 4, while Table 1 contains the selected bond lengths and angles and Figures 1 and 2 exhibit ORTEP views of the molecules. Data processing was performed using the WinGX package[40]. The structures were solved by direct methods using SIR-2004[41] and refined by least squares on F^2 with anisotropic displacement parameters for non-H atoms using SHELXL97[42]. All hydrogen atoms were located from difference Fourier maps and refined as riding on their parent atoms. Crystallographic data for the structures reported in this paper have been deposited in the Cambridge Crystallographic Data Centre as supplementary publication, CCDC No. 882.688 and Nº 882.689 for compounds (**7**) and (**17**), respectively. Copies of this information may be obtained free of charge from The Director, CCDC, 12 Union Road, Cambridge CB2 1EZ, UK. Fax: +44 1223 336 033. E-mail: data_request@ccdc.cam.ac.uk. Web page: http://www.ccdc.cam.ac.uk.

Table 4. Crystal data and structure refinement parameters of the compounds (**7**) and (**17**).

	7	**17**
Empirical formula	$C_{11}H_{10}Br_1N_{12}O_1$	$C_{11}H_{10}N_4O_3$
Formula weight	280.12	246.23 g/mol
Temperature	294(2) K	294(2) K
Wavelength	0.71073 Å	0.71073 Å
Crystal system	Monoclinic	Monoclinic
Space group	$P2_1/n$	C2/c
Unit cell dimensions	a = 13.5334(6) Å, α= 90°	a = 11.765(4) Å , α= 90°

View Article Online
DOI: 10.1039/C4NJ02427C

	b = 12.3004(8) Å, β= 102.177(6)°	b = 11.314(6) Å, β= 95.75(4)°
	c = 28.098(2) Å γ = 90°	c = 17.774(12) Å, γ= 90°
Volume	4572.1(5) Å3	2354(2) Å3
Z	16	8
Density (calculated)	1.628 Mg/m3	1.390 Mg/m3
Absorption coefficient	3.578 mm-1	0.105 mm-1
F(000)	2240	1024
Crystal size	0.42 x 0.36 x 0.12 mm3	0.38 × 0.34 × 0.23 mm3
θ range for data collection	2.88 to 29.36°	2.30 to 25.98°
Index ranges	$-17 \le h \le 18$, $-16 \le k \le 15$, $-38 \le l \le 38$	$-14 \le h \le 14$, $0 \le k \le 13$, $0 \le l \le 21$
Reflections collected	50022	2703
Independent reflections	11446 [R(int)= 0.0931]	2303 [R(int) = 0.0553]
Completeness to	θ = 29.36°, 91.0 %	θ = 25.98°, 100.0%
Refinement method	Full-matrix least-	Full-matrix least-

View Article Online
DOI: 10.1039/C4NJ02427C

	squares on F2	squares on *F2*
Data/restraints/parameters	11446/246/594	2303/0/165
Goodness-of-fit on *F2*	1.056	1.017
Final R indices [$I > 2\sigma(I)$]	R1= 0.0789, *w*R2= 0.1448	R1= 0.0576, *w*R2= 0.1374
R indices (all data)	R1= 0.1773, *w*R2= 0.1790	R1= 0.1436, *w*R2= 0.1615
Largest diff. peak and hole	0.574 and -0.555 e·Å-3	0.216 and -0.150 e·Å-3

4.4. Pauling's bond orders, n, and conjugation parameters, η.

The π-electronic delocalization on the fragment C(2)-C(1)-N(1)-N(2)-C(6) of compounds (**7b**)-(**7d**) and (**17**) was evaluated in terms of Pauling's bond order, *n*, taking three separated sub fragments, C(2)-C(1)-N(1), C(1)-N(1)-N(2) and N(1)-N(2)-C(6), for obtaining the η paremeters. The standard single bond length in crystalline state found in C_2H_6, $d_{C\text{-}C}$: 1,513 Å, CH_3NH_2, $d_{C\text{-}N}$: 1.469 Å and NH_2NH_2, $d_{N\text{-}N}$: 1.425 Å; were obtained from literature[26,27] and the corresponding crystallographic data from the Table 1. These data were used for obtaining n_1 in C(2)-C(1); n_2 in C(1)-N(1); n_3 in N(1)-N(2) and n_4 in N(2)-C(6) using the Pauling's equation, [43] $-\Delta R(n)/2 = 0.353\log n$. Conjugation parameters, η, were evaluated in terms of percentage, as $\%\eta_{1,2} = ½[(2-n_1)+(n_2-1)]\times100$, $\%\eta_{2,3} = ½[(2-n_2)+(n_3-1)]\times100$ and $\%\eta_{3,4} = ½[(2-n_3)+(n_4-1)]\times100$, were $\eta_{1,2}$, $\eta_{2,3}$ and $\eta_{3,4}$ are by definition equal to 0, 1 and 0.5 for non-delocalized C=C-N=N-C, ionic $^{+}$C-C=N-N=C^{-}

View Article Online
DOI: 10.1039/C4NJ02427C

and fully delocalized fragment C≡C≡N≡N≡C, respectively. The results are shown in Table 3 and compared with the analogous fragment of the compound (**18**) available in literature[23]. Because of the disorder found in the crystallographic data of the molecule (**7a**) the corresponding data were not considered in these calculations.

4.5. Synthesis

In a 100 mL round-bottomed flask were added: 0.01 mole of any β-diketohydrazone, *R*-C_6H_4-NHN=C($COCH_3$)$_2$ {*m*, *R*= 2,47 g, *4*-N(CH_3)$_2$(**1**); 2.20 g, *4*-OH(**2**); 2.18 g, *4*-CH_3(**3**); 2.34 g, *4*-OCH_3(**4**); 2.04 g, *4*-H(**5**); 2.39 g, *4*-Cl(**6**); 2.83 g, *4*-Br(**7**); 2.48 g, *4*-CO_2H(**8**); 2.76 g, *4*-$CO_2CH_2CH_3$(**9**); 2.46 g, *4*-$COCH_3$(**10**); 2.29 g, *4*-CN(**11**); 2.49 g, *4*-NO_2(**12**); 2.90 g, *4*-$CH_2CO_2CH_2CH_3$(**13**); 2.39 g, 3-Cl(**14**); 2.20 g, 2-OH(**15**); 2.39 g, 2-Cl(**16**); 2.49 g, 2-NO_2(**17**)}; 2.48, 2-CO_2H(**18**)}, 30 mL de ethanol, 2 mL of glacial acetic acid and 0.01 mole (0.69 g) of $NH_2OH{\cdot}HCl$. The reaction mixture was heated at reflux temperature stirring magnetically during 18 h. For precipitation of each compound the mixture was cooled to room temperature and then cooled at -18 ºC during 2 h or by addition of around 25 mL of water. The yellow-orange solids were filtered by suction, washed with abundant quantity of water and dried under vacuum at 40 ºC by 24 h. All compounds were recrystallized from ethanol/H_2O mixtures of variable composition. Compound (**13**) may be also recrystallized from a 5:1 acetone/H_2O. Finally, compounds (**7**) and (**17**) yield single crystals suitable for X-ray studies by recrystallization from 3:1 and 2:1 EtOH/H_2O mixtures, respectively.

View Article Online
DOI: 10.1039/C4NJ02427C

4.6. Analysis

4.6.1. Compound (**1**) *(E)-4-((3,5-dimethylisoxazol-4-yl)diazenyl)-N,N-dimethylaniline*: Yield: 39 %. Recryst. from EtOH/H_2O 2:1. MP: 129-130 ºC. EA: for $C_{13}H_{16}N_4O$ (Mɪ: 244.29 g/mole): Calc(%): C, 63.91; H, 6.60; N, 22.93; Found(%): C, 63.83; H, 6.69; N, 22.78. UV-vis in EtOH 4.09×10^{-5} mole/L, λ_{max}, nm(logε): 423sh; 392(4.18); 328(3.47); 315(3.45); 262(3.93). IR, ν(cm^{-1}): ν(R-H): 2986w, 2908m, 2818w; ν(N=N) or ν(C=N): 1600s; ν(C=C): 1561m, 1517m; ν(N-O): 1409m. ^{1}H NMR (495 MHz in *$CDCl_3$*) δ ppm: 2.52 (s, 3H, H_1), 2.70 (s, 3H, H_5), 3.07 (s, 6H, N(C**H$_3$**)$_2$), 6.77-6.69 (m, 2H, Ar-H) 7.80 – 7.69 (m, 2H, Ar-H). ^{13}C NMR (495 MHz in *$CDCl_3$*) δ ppm: C_1: 12.10; C_2: 154.36; C_3: 132.34; C_4:166.49; C_5: 11.72; C_6, C_9: 144.05, 152.28; C_7, C_8: 124.12. 111.57; C_R: 40.40 N(**C**H$_3$)$_2$.

4.6.2. Compound (**2**) *(E)-4-((3,5-dimethylisoxazol-4-yl)diazenyl)phenol*: Yield: 92 %. Recryst. from EtOH/H_2O 2:1. MP: 170-171 ºC. EA: for $C_{11}H_{11}N_3O_2$ (Mɪ: 217.22 g/mole): Calc(%): C, 60.82; H, 5.10; N, 19.34; Found(%): C, 60.81; H, 5.23; N, 19.26. UV-vis in EtOH 4.72×10^{-5} mole/L, λ_{max}, nm(logε): 420sh; 346(4.35); 246(4.09). IR, ν(cm^{-1}): ν(O-H): 3142s; ν(Ar-H): 3087w, 3030w; ν(R-H): 2942w, 2841w; ν(N=N) or ν(C=N): 1617s; ν(C=C): 1586s y 1508m; ν(N-O): 1411s. ^{1}H NMR (495 MHz in *DMSO-d_6*) δ ppm: 2.43 (s, 3H, H_1), 2.70 (s, 3H, H_5), 6.94-6.87 (m, 2H, Ar-H), 7.74-7.66 (m, 2H, Ar-H), 10.22 (s, 1H, H_R (-O**H**)). ^{13}C NMR (495 MHz in *DMSO-d_6*) δ ppm: C_1: 11.64; C_2: 153.14; C_3: 131.45; C_4: 168.03, C_5: 11.25; C_6, C_9: 145.54, 160.56; C_7, C_8: 124.09, 115.84.

View Article Online
DOI: 10.1039/C4NJ02427C

4.6.3. Compound (**3**) *(E)-3,5-dimethyl-4-(p-tolyldiazenyl)isoxazole*: Yield: 93 %. Recryst. from EtOH/H_2O 2:1. MP: 78-79 ºC. EA: for $C_{12}H_{13}N_3O$ (Mι: 215.25 g/mole) Calc(%): C, 66.96; H, 6.09; N, 19.52. Found(%): C, 67.04; H, 6.18; N, 19.58. UV-vis in EtOH 6.37×10^{-5} mole/L, λ_{max}, nm (log**ε**): 423(2.93); 323(4.30); 312sh; 240(4.03); 234(4.06); 228sh. IR, ν(cm^{-1}): ν(Ar-H): 3087w, 3026w; ν(R-H): 2992w, 2923w; ν(N=N) or ν(C=N): 1610s; ν(C=C): 1589m y 1497m; ν(N-O): 1407s. ^{1}H NMR (495 MHz in *$CDCl_3$*) δ ppm: 2.42 (s, 3H, H_R (C**H_3**-)), 2.53 (s, 3H, H_1), 2.74 (s, 3H, H_5), 7.30-7.27 (m, 2H, Ar-H), 7.71 (d, *J* = 8.30 Hz, 2H, Ar-H). ^{13}C NMR (495 MHz in *$CDCl_3$*) δ ppm: C_1: 12.19; C_2: 153.99; C_3: 132.50; C_4: 168.92; C_5: 11.79; C_6, C_9: 141.36, 151.17; C_7, C_8: 122.28, 129.83; C_R: 21.58.

4.6.4. Compound (**4**) *(E)-4-((4-methoxyphenyl)diazenyl)-3,5-dimethylisoxazole*: Yield: 99%. Recryst. from EtOH/H_2O 2:1. MP: 107-108 ºC. EA: for $C_{12}H_{13}N_3O_2$ (Mι: 231.25 g/mole) Calc(%): C, 62.33; H, 5.67; N, 18.17; Found(%): C, 62.52; H, 5.82; N, 18.22. UV-vis in EtOH 4.58×10^{-5} mole/L, λ_{max}, nm(log**ε**): 405sh; 346sh; 337(4.36); 242(4.15). IR, ν(cm^{-1}); ν(Ar-H): 3070w, 3039w; ν(R-H): 2965w, 2934w, 2841w; ν(N=N) or ν(C=N): 1601s; ν(C=C): 1579s, 1497s; ν(N-O): 1407s. ^{1}H NMR (495 MHz in *$CDCl_3$*) δ ppm: 2.52 (s, 3H, H_1), 2.72 (s, 3H, H_5), 3.88 (s, 3H, H_R (C**H_3**O-)), 7.02 – 6.94 (m, 2H, Ar-H) 7.86 – 7.72 (m, 2H, Ar-H). ^{13}C NMR (495 MHz in *$CDCl_3$*) δ ppm C_1: 12.20: C_2: 154.09; C_3: 132.40; C_4: 168.30; C_5: 11.79; C_6, C_9: 147.45, 161.96; C_7, C_8: 114.33, 124.10, C_R: 55.73.

4.6.5. Compound (**5**) *(E)-3,5-dimethyl-4-(phenyldiazenyl)isoxazole*: Yield: 65 %. Recryst. in EtOH/H_2O 3:1.MP: 44-45 ºC. EA:for $C_{11}H_{11}N_3O$ (Mι: 201.22 g/mole) Calc(%): C, 65.66; H, 5.51; N, 20.88; Found(%): C, 65.96; H, 5.59; N, 20.98. UV-vis in EtOH 5.19×10^{-5} mole/L, λ_{max}, nm(log**ε**): 425(2.75); 317(4.23); 308sh(4.22); 233sh(3.98); 228(4.03); 222sh(4.00). IR, ν(cm^{-1}):

View Article Online
DOI: 10.1039/C4NJ02427C

ν(Ar-H): 3083w, 3042w; ν(R-H): 2988w, 2925m; ν(N=N) or ν(C=N): 1611f; ν(C=C): 1592m y 1504w; ν(N-O): 1412s. ^{1}H NMR (495 MHz in *CDCl$_3$*) δ ppm: 2.54 (s, 3H, H_1), 2.75 (s, 3H, H_5), 7.52-7.38 (m, 3H, Ar-H), 7.83-7.78 (m, 2H, Ar-H). ^{13}C NMR (495 MHz in *CDCl$_3$*) δ ppm: C_1: 12.15; C_2: 153.84; C_3: 132.55; C_4: 169.42; C_5: 11.75; C_6, C_9: 130.79, 152.99; C_7, C_8: 122.27; 129.14.

4.6.6. Compound (**6**) *(E)-4-((4-chlorophenyl)diazenyl)-3,5-dimethylisoxazole*: Yield: 98 %. Recryst. in EtOH/H_2O 3:1. MP: 56-57 ºC. EA: for $C_{11}H_{10}ClN_3O$ (Mι: 235.67 g/mole) Calc(%): C, 56.06; H, 4.28; N, 17.83; Found(%): C, 56.13; H, 4.54; N, 17.86. UV-vis in EtOH 5.13×10^{-5} mole/L, λ_{max}, nm(log**ε**): 424(2.86); 324(4.35); 313sh; 239sh; 233(4.08); 227sh. I R, ν(cm^{-1}): ν(Ar-H): 3068w; ν(R-H): 2982w, 2929w; ν(N=N) or ν(C=N): 1612s; ν(C=C): 1590m, 1576w; ν(N-O): 1403s. ^{1}H NMR (400 MHz in *CDCl$_3$*) δ ppm: 2.52 (s, 3H, H_1), 2.75 (s, 3H, H_5), 7.56-7.35 (m,2H, Ar-H), 7.94-7.6 (m, 2H, Ar-H). ^{13}C NMR (400 MHz in *CDCl$_3$*) δ ppm: C_1: 12.25; C_2: 153.78; C_3: 132.60; C_4: 169.93; C_5: 11.84; C_6, C_9: 136.71, 151.40; C_7, C_8: 123.59, 129.46.

4.6.7. Compound (**7**) *(E)-4-((4-bromophenyl)diazenyl)-3,5-dimethylisoxazole***:** Yield: 91 %. Recryst. in EtOH/H_2O 3:1 yields single crystals. MP: 89-90. EA: for $C_{11}H_{10}BrN_3O$ (Mι: 280.12 g/mole): Calc(%): C, 47.16; H, 3.60; N, 15.00; Found(%): C, 47.20; H, 3.75; N, 14.94. UV-vis in EtOH 5.09×10^{-5} mole/L, λ_{max}, nm(log**ε**): 4.25(2.96); 325(4.35); 315sh; 240sh; 234(4.03); 227sh. IR, ν(cm^{-1}); ν(Ar-H): 2974w, 2932w; ν(N=N) or ν(C=N): 1605s; ν(C=C): 1584m y 1569m; ν(N-O): 1407s. ^{1}H NMR (495 MHz in *CDCl$_3$*) δ ppm: 2.52 (s, 3H, H_1), 2.75 (s, 3H, H_5), 7.64-7.58 (m, 2H, Ar-H), 7.71-7.65 (m, 2H, Ar-H). ^{13}C NMR (495 MHz in *CDCl$_3$*) δ ppm: C_1: 12.23; C_2: 153.77; C_3: 132.63; C_4: 169.98; C_5: 11.86; C_6, C_9: 125.12, 151.77; C_7, C_8: 123.83, 132.44.

View Article Online
DOI: 10.1039/C4NJ02427C

4.6.8. Compound (**8**) *(E)-4-((3,5-dimethylisoxazol-4-yl)diazenyl)benzoic acid***:** Yield: 89 %. Recryst. from EtOH/H_2O 2:1. MP: 108-109 ºC. AE: for $C_{12}H_{11}N_3O_3$ (Mι: 245.23 g/mole). Calc(%): C, 58.77; H, 4,52; N, 17.13; Found(%): C, 59.81; H, 4.92; N, 16.47. UV-vis in EtOH 4.79×10^{-5} mole/L, λ_{max}, nm(log**ε**): 432(2.88); 322(4.28); 233sh; 227(3.89); 221sh. IR, ν(cm^{-1}): ν(O-H): 3284-2175s, ν(C=O): 1674s; ν(C=C): 1597s, 1581m, 1505w; ν(N-O): 1410s. ^{1}H NMR (495 MHz in *DMSO-d_6*) δ ppm 2.47 (s, 3H, H_1), 2.78 (s, 3H, H_5), 7.91-7.88 (m, 2H, Ar-H), 8.14-8.09 (m, 2H, Ar-H), 13.16 (s, 1H, H_R (COO**H**)). ^{13}C NMR (495 MHz in *DMSO-d_6*) δ ppm: C_1: 11.71; C_2: 152.84; C_3: 132.17; C_4: 171.26; C_5: 11.43; C_6, C_9: 132.48, 154.66; C_7, C_8:122.02, 130.58; C_R: 166.70 (>**C**OOH).

4.6.9. Compound (**9**) *(E)-ethyl 4-((3,5-dimethylisoxazol-4-yl)diazenyl)benzoate***:** Yield: 67 %. Recryst. from EtOH/H_2O 2:1. MP: 107-108 ºC. EA: for $C_{14}H_{15}N_3O_3$ (Mι: 273.29 g/mole) Calc(%): C, 61.53; H, 5.53; N, 15.38. Found(%): C, 61.93; H, 5.98; N, 15.18. UV-vis in EtOH 4.67×10^{-5} mole/L, λ_{max}, nm(log**ε**): 429(2.92); 332(4.32); 233sh; 227(3.94), 220sh. IR, ν(cm^{-1}): ν(R-H): 2986w, 2954w; ν(C=O): 1715s; ν(N=N) or ν(C=N): 1611w; ν(C=C): 1598s; ν(N-O): 1409s. ^{1}H NMR (400 MHz in *DMSO-d_6*) δ ppm: 1.34 (t, 3H, (C**H$_3$**CH_2-)), 2.46 (s, 3H, H_1), 2.77 (s, 3H, H_5), 4.34 (q, 2H, (CH_3C**H$_2$**-)), 7.89 (d, *J* = 8.4 Hz, 2H, Ar-H), 8.11 (d, *J* = 8.5 Hz, 2H, Ar-H). ^{13}C NMR (400 MHz in *DMSO-d_6*) δ ppm: C_1: 11.68; C_2: 154.75; C_3: 132.17; C_4: 171.36; C_5: 11.41; C_6, C_9: 131.41, 154.75, C_7, C_8: 122.11, 130.38; C_R: 14.12 (**C**H_3CH_2-), 61.05, (CH_3**C**H_2-), 165.09 (-**C**OOR).

4.6.10. Compound (**10**) *(E)-1-(4-((3,5-dimethylisoxazol-4-yl)diazenyl)phenyl)ethanone*: Yield: 99 %. Recryst. from EtOH/H_2O 2:1. MP: 106-107 ºC. EA: for $C_{13}H_{13}N_3O_2$ (Mι: 243.26 g/mole) Calc(%): C, 64.19; H, 5.39; N, 17.27; Found(%): C, 62.79; H, 5.77; N, 19.54. UV-vis in EtOH 4.77×10^{-5} mole/L, λ_{max}, nm(log**ε**): 427(3.02); 330(4.34); 229(4.01). IR, ν(cm^{-1}): ν(Ar-H): 3038w;

View Article Online
DOI: 10.1039/C4NJ02427C

ν(R-H): 2992w, 2929w; ν(C=O): 1652s; ν(C=C): 1595s; 1498w; ν(N-O): 1401s. ^{1}H NMR (400 MHz in *$CDCl_3$*) δ ppm 2.54 (s, 3H, H_1), 2.66 (s, 3H, H_R, (C**H**$_3$CO-)), 2.78 (s, 3H, H_5), 7.89-7.84 (m, 2H, Ar-H$_r$), 8.11-8.05 (m, 2H, Ar-H). ^{13}C NMR (400 MHz in *$CDCl_3$*) δ ppm: C_1: 12.25; C_2: 153.27; C_3: 132.77; C_4: 170.84; C_5: 11.91; C_6, C_9: 138.30, 155.48; C_7, C_8: 122.41, 129.51; C_R: 26.94 (**C**H$_3$C=O), 197.57 (CH$_3$**C**=O).

4.6.11. Compound (**11**) *(E)-4-((3,5-dimethylisoxazol-4-yl)diazenyl)benzonitrile***: Y**ield: 79 %. Recryst. from EtOH/H_2O 2:1. MP: 141-142 ºC. EA: for $C_{12}H_{10}N_4O$ (Mt: 226.23 g/mole) Calc(%): C, 63.71; H, 4.46; N, 24.76. Found(%): C, 63.92; H, 4.77; N, 24.98. UV-vis in EtOH 5.00×10^{-5} mole/L, λ_{max}, nm(log**ε**): 432(2.84); 321(4.27); 234sh; 227(3.91); 222sh. IR, ν(cm^{-1}): ν(Ar-H): 3095d; ν(R-H): 2985w, 2924; ν(C≡N): 2225s; ν(N=N) or ν(C=N): 1613s; ν(C=C): 1597s; ν(N-O): 1407s. ^{1}H NMR (400 MHz in *$CDCl_3$*) δ ppm: 2.53 (s, 3H, H_1), 2.78 (s, 3H, H_5), 7.79 (d, *J* = 8.4 Hz, 2H, Ar-H), 7.88 (d, *J* = 8.4 Hz, 2H, Ar-H). ^{13}C NMR (400 MHz in *$CDCl_3$*) δ ppm: C_1: 12.29; C_2: 153.45; C_3: 133.05; C_4: 171.57; C_5: 11.94; C_6, C_9: 118.59, 154.92; C_7, C_8: 122.89, 133.35; C_R: 113.79 (C≡N).

4.6.12. Compound (**12**) *(E)-3,5-dimethyl-4-((4-nitrophenyl)diazenyl)isoxazol*: Yield: 88 %. Recryst. from EtOH/H_2O 2:1. MP: 152-153 ºC. EA: for $C_{11}H_{10}N_4O_3$ (Mt: 246.22 g/mole). Calc(%): C, 53.66; H, 4.09; N, 22.75; Found: C, 53.81; H, 5.15; N, 22.79. UV-vis in EtOH 4.75×10^{-5} mole/L, λ_{max}, nm(log*ε*): 433(3.00); 329(4.34); 217(4.11). IR, ν(cm^{-1}): ν(Ar-H): 3101w , 3060w; ν(R-H): 2995w 2929w; ν(N=N) or ν(C=N): 1607s; ν(C=C): 1583m, 1518m; ν(N-O): 1407s. ^{1}H NMR (495 MHz in *$CDCl_3$)* δ ppm 2.54 (s, 3H, H_1), 2.80 (s, 3H, H_5), 7.95-7.89 (m, 2H, Ar-H), 8.39-8.32 (m, 2H, Ar-H). ^{13}C NMR (495 MHz in *$CDCl_3$*) δ ppm: C_1: 12.28; C_2: 153.42; C_3: 133.24; C_4: 171.90; C_5: 11.98; C_6, C_9: 148.65, 156.19; C_7, C_8: 122.95, 124.89.

View Article Online
DOI: 10.1039/C4NJ02427C

4.6.13. Compound (**13**) *(E)-ethyl 2-(4-((3,5-dimethylisoxazol-4-yl)diazenyl)phenyl)acetate***:** Yield: 92 %. Recryst. from EtOH/H_2O 2:1. MP: 79-80 ºC. EA: for $C_{15}H_{17}N_3O_3$ (Mι: 287.31 g/mol) Calc. (%): C, 62.71; H, 5.96; N, 14.63. Enc. (%): C, 62.70; H, 6.08; N, 14.63. UV-vis 4.53×10^{-5} mole/L, λ_{max}, nm(log**ε**): 418(2.90); 322(4.29); 311sh; 238sh; 231(4.03); 225sh. IR, ν(cm^{-1}): ν(Ar-H): 3046w; ν(R-H): 2989w, 2926w; ν(C=O): 1726s; ν(N=N) or ν(C=N): 1612s; ν(C=C): 1592w, 1504d; ν(N-O): 1414s. For the compound recrystallized in acetone the ^{1}H NMR (495 MHz in *$CDCl_3$*) δ ppm: 1.26 (t, *J*= 7.14 Hz, 3H, H_R (C**H$_3$**CH_2-)), 2.17 (s, 6H, solvent (C**H$_3$**)$_2$CO)), 2.52 (s, 3H, H_1), 2.74 (s, 3H, H_5), 3.68 (s, 2H, H_R (-C**H$_2$**-)), 4.17 (q, *J*= 7.15 Hz, 2H, H_R (CH_3C**H$_2$**-)), 7.41 (d, *J*= 8.33 Hz, 2H, Ar-H), 7.77 (d, *J*= 8.37 Hz, 2H, Ar-H). ^{13}C NMR (495 MHz in *$CDCl_3$*) δ ppm: C_1: 12.20; C_2: 153.89; C_3: 132.61; C_4: 169.42; C_5: 11.81; C_6, C_9: 137.06, 152.12; C_7, C_8: 122.50, 130.15; C_R: 14.30 (**C**H_3CH_2-); 41.39 (-**C**H_2-); 61.18 (CH_3**C**H_2-); 171.23 (>**C**OOR), $C_{Solv.}$: 31.05 (**C**H_3)$_2$CO); 207.02 (CH_3)$_2$**C**O).

4.6.14. Compound (**14**) *(E)-4-((3-chlorophenyl)diazenyl)-3,5-dimethylisoxazole*: Yield: 71 %. Recryst. from EtOH/H_2O 3:1. MP: 74-75 ºC. EA: for $C_{11}H_{10}ClN_3O$ (Mι: 235.67 g/mol), Calc(%): C, 56.06; H, 4.28; N, 17.83; Found(%): C, 56.16; H, 4.45; N, 17.89. UV-vis in EtOH 4.56×10^{-5} mole/L, λ_{max}, nm(log**ε**): 425(2.77); 315(4.23); 238sh; 231(4.05); 226(4.03). IR, ν(cm^{-1}): ν(Ar-H,): 3090w, 3076w; ν(R-H): 2925w; ν(N=N) or ν(C=N): 1610s; ν(C=C): 1587m, 1575m, 1504w; ν(N-O): 1409s. ^{1}H NMR (495 MHz in $CDCl_3$) δ ppm 2.52 (s, 3H, H_1), 2.76 (s, 3H, H_5), 7.45-7.39 (m, 2H, Ar-H), 7.71 (dt, *J* = 7.04, 1.94 Hz, 1H, Ar-H), 7.81-7.75 (m, 1H). ^{13}C NMR (495 MHz in *$CDCl_3$*) δ ppm: C_1: 12.24; C_2: 153.70; C_3: 132.63; C_4: 170.40; C_5: 11.87; C_6, C_{10}: 135.28, 153.86; C_7, $C_{8,}$ C_9, C_{11}: 121.33, 121.82, 130.26, 130.55.

View Article Online
DOI: 10.1039/C4NJ02427C

4.6.15. Compound (**15**) *(E)-2-((3,5-dimethylisoxazol-4-yl)diazenyl)phenol*: Yield: 24 %. Recryst. from EtOH/H_2O 3:1. MP: 110-111 ºC. EA: for $C_{11}H_{11}N_3O_2$ (Mt: 217.22 g/mole), Calc(%): C, 60.82; H, 5.10; N, 19.34; Found(%): C, 61.20; H, 5.35; N, 19.15. UV-vis in EtOH 5.06×10^{-5} mole/L, λ_{max}, nm(log**ε**): 412sh; 368(3.99); 316(4.22); 247(3.79); 214(3.62). IR, ν(cm^{-1}): ν(O-H): 3270-2700s; ν(N=N) or ν(C=N): 1619s; ν(C=C): 1582s, 1511w; ν(N-O): 1416s. ^{1}H NMR (495 MHz in *DMSO-d_6*) δ ppm: 2.47 (s, 3H, H_1), 2.73 (s, 3H, H_5), 6.97-6.92 (m, 1H, Ar-H), 7.07-7.03 (m, 1H, Ar-H), 7.39-7.34 (m, 1H, Ar-H), 7.62-7.58 (m, 1H, Ar-H), 10.37 (s, 1H, OH). ^{13}C NMR (495 MHz in *DMSO-d_6*) δ ppm: C_1: 11.46; C_2: 153.38; C_3: 131.74; C_4: 168.52; C_5: 11.41; C_6, C_{11}: 139.5; 154.24; C_7, C_8, C_9, C_{10} : 118.04, 119.61, 120.20, 132.86.

4.6.16. Compound (**16**) *(E)-4-((2-chlorophenyl)diazenyl)-3,5-dimethylisoxazole*: Yield: 82 %. Recryst. from EtOH/H_2O 2:1. MP: 116-117 ºC. EA: for $C_{11}H_{10}ClN_3O$ (Mt: 235.67 g/mole), Calc(%): C, 56.06; H, 4.28; N, 17.83; Found(%): C, 56.08; H, 4.41; N, 17.85. UV-vis in EtOH 4.71×10^{-5} mole/L, λ_{max}, nm(log**ε**): 429(2.82); 319(4.20); 241sh; 235(4.02); 229sh. IR, ν(cm^{-1}): ν(Ar-H): 3065w; ν(R-H): 2992w, 2931w; ν(N=N) or ν(C=N): 1610s; ν(C=C): 1586m, 1503w; ν(N-O): 1408s. ^{1}H NMR (495 MHz in *$CDCl_3$*) δ ppm: 2.57 (s, 3H, H_1), 2.78 (s, 3H, H_5), 7.32 (td, *J* = 7.6, 1.8 Hz, 1H, Ar-H), 7.37 (td, *J* = 7.6, 1.5 Hz, 1H, Ar-H), 7.55 (dd, *J* = 7.8, 1.5 Hz, 1H, Ar-H), 7.66 (dd, *J* = 7.9, 1.8 Hz, 1H, Ar-H). ^{13}C NMR (495 MHz in *$CDCl_3$*) δ ppm: C_1: 12.29; C_2: 153.99; C_3: 133.50; C_4: 170.31; C_5: 11.92; C_6, C_{11}: 135.31, 148.95; C_7, C_8, C_9, $C_{10:}$ 116.83, 127.34 130.83, 131.62.

4.6.17. Compound (**17**) *(E)-3,5-dimethyl-4-((2-nitrophenyl)diazenyl)isoxazole*: Yield: 86 %. Recryst. in EtOH/H_2O 2:1 yields single crystals. MP: 138-139 ºC. EA: for $C_{11}H_{10}N_4O_3$ (Mt: 246.22 g/mole) Calc(%) C, 53.66; H, 4.09; N, 22.75; Found(%): C, 53.95; H, 4.18; N, 22.84. UV-vis in

View Article Online
DOI: 10.1039/C4NJ02427C

EtOH 4.87×10^{-5} mole/L, λ_{max}, nm(logε): 424(2.71); 319(4.25); 221(4.14). IR, $\nu(cm^{-1})$: ν(Ar-H): 3092w, 3016w; ν(R-H): 2931w; ν(N=N) or ν(C=N): 1606s; ν(C=C): 1524s, 1474w; ν(N-O): 1406m. ^{1}H NMR (495 MHz in *$CDCl_3$*) δ ppm: 2.46 (s, 3H), 2.76 (s, 3H), 7.60-7.51 (m, 1H, Ar-H), 7.69-7.61 (m, 2H, Ar-H), 7.91-7.82 (m, 1H, Ar-H). ^{13}C NMR (495 MHz in *$CDCl_3$*) δ ppm: C_1: 12.08; C_2: 153.75; C_3: 133.45; C_4: 171.74; C_5: 11.92; C_6, C_{11}: 145.38, 147.79; C_7, C_8, C_9, C_{10}: 117.97, 124.05 130.54, 132.92.

4.6.18. Compound (18) *(E)-2-((3,5-dimethylisoxazol-4-yl)diazenyl)benzoic acid*: Yield: 84 %. Recryst. from EtOH/H_2O 3:1. MP: desc.>160 ºC. EA: for $C_{12}H_{11}N_3O_3$ (Mt: 245.23 g/mole); Calc(%): C, 58.77; H, 4.52; N, 17.13; Found(%): C, 58.79; H, 4.82; N, 17.04. UV-vis EtOH 5.04×10^{-5} mole/L λ_{max}, nm(logε): 420(2.70); 313(4.19); 233sh; 217(4.10). IR, $\nu(cm^{-1})$: ν(O-H): 3230-2360s; ν(C=O): 1694s; ν(N=N) or ν(C=N): 1610m; ν(C=C): 1593m, 1509w; ν(N-O): 1413s. ^{1}H NMR (495 MHz in *DMSO-d_6*) δ ppm: 2.42 (s, 3H), 2.75 (s, 3H), 7.67-7.52 (m, 3H, Ar-H), 7.77-7.70 (m, 1H, Ar-H), 13.23 (bs, 1H, OH). ^{13}C NMR (495 MHz in *DMSO-d_6*) δ ppm: C_1: 11.47; C_2: 152.92; C_3: 132.17; C_4: 170.75; C_5: 11.26; C_6, C_{11}: 131.16, 150.35; C_7, C_8, C_9, C_{10}: 117.07, 128.88, 130.33, 131.39; C_R: 168.57 (COOH).

4.7 Biological studies

4.7.1. Tissue Culture: The HL-60, *promyelocytic leukemia* cell line, was purchased from the American Type Culture Collection-ATCC (Manassas, VA). This cell line was collected from peripheral blood cells of a 36-year old Caucasian female with acute *promyelocytic leukemia* (APL) and they grow as a suspension culture. The predominant cell population consists of neutrophilic

View Article Online
DOI: 10.1039/C4NJ02427C

promyelocytes[44,45]. In the laboratory, these cells were stored under liquid nitrogen until use. Then, they were thawed by gentle stir of their containers (vials) during 2 minutes in a water bath at 37 ºC. After thawing, the content of each vial of cells was transferred into a 25 cm^2 tissue culture flask, T-25, diluting with 10 mL of RPMI 1640 containing 1 mmol/L L-glutamine (GIBCO/BRL, Gaithersburg, MD), supplemented with 10% (v/v) of fetal bovine serum (FBS) and 1% (w/v) penicillin/streptomycin. The T-25 flasks (2 x 10^6 viable cells) was observed under the microscope, followed by incubation in a humidified 5 % CO_2 at 37 °C. Three times a week, the culture cells was diluted under same conditions in order to maintain a density of 5 x 10^5 cells/mL and harvested in the exponential phase of growth. The cell viability was assessed by the Trypan Blue exclusion test (Life Technologies) and manually counted using a hemocytometer.

4.7.2. Cytotoxicity/MTT Assay: This colorimetric assay measures the reduction of 3-(4,5-dimethylthiasol-2-yl)-2,4,-diphenyltetrazolium bromide (MTT) by mitochondrial succinate dehydrogenase. The MTT enters the cells and passes to the mitochondria where is reduced to formazan, an insoluble colored product. In order to dissolve the formazan, the cells are then treated with an organic solvent (DMSO or isopropanol) and the obtained solution is measured spectrophotometrically between 530-650 nm range[46,47].

Aliquots of 200 µL of HL-60 cell suspension (5x 10^5 cells/mL) were seeded into 96 well polystyrene tissue culture plates, an aliquot of 1.0 µL of isoxazole (2.0, 5.0, 8.0, 12.0, 20.0, 30.0, 40.0, 60.0, 80.0 and 100.0 µM) and, carefully, were also added to each well using DMSO:EtOH (1:4) as solvent and vehicle control. Cells incubated in culture medium alone served as a control for cell viability (untreated wells). Cells were placed in the humidified 5% CO_2 incubator at 37°C for 24 hours. After incubation, 10 µL aliquots of MTT solution (5 mg/mL in PBS) were added to each well and re-incubated for 4 hours at 37° C, followed by low centrifugation at 800 rpm for 5

View Article Online
DOI: 10.1039/C4NJ02427C

minutes. Then, the 200 µL of supernatant culture medium were carefully aspirated and 200 µL aliquots of dimethylsulfoxide (*DMSO*) were added to each well in order to dissolve the formazan crystals, followed by incubation during 10 minutes. The culture plate was placed on an E_{max} model micro-plate reader (Molecular Devices) and the absorbance was measured using a 650 nm filter. The amount of color produced is directly proportional to the number of viable cells. All assays were performed four times with three replicates each one processed independently and means ± SD values were used to estimate the cell viability. Cell viability rate was calculated as the percentage of MTT absorption as follows:

$$\% \text{ survival} = (\text{mean experimental absorbance/mean control absorbance}) \times 100.$$

The isoxazole concentration was plotted against the corresponding percentage (%) of cell viability obtained with MTT assays, and the 50% inhibitory concentration (IC_{50}) was calculated by non-linear regression using fitting with Sigmaplot©11 program from Systat Software, Inc.

4.7.3. Semiquantitive duplex RT-PCR: Total RNA was isolated from cells using Chomczynski's method[48] and quantified by measuring of its optical density at 260 nm. First strand *c*DNA was synthesized with 2 µg of total RNA in a buffer containing 100 pmol of oligo dT, dNTPs 0.25 mM, DTT 10 mM, 20U of RNase Inhibitor and 50U of M-MLV Reverse Transcriptase (Invitrogen). The mixture was incubated for 1 h at 42◦ C. The PCR amplifications were carried out using GoTaq Green Master Mix (Promega). For quantitative analysis of Bcl-2, p21WAF1, and Bax mRNAs, human glyceraldehyde-3-phosphate dehydrogenase (G3PDH) gene served as the internal control for calculation of the densitometry results. The primers were designed based on the sequences of the

View Article Online
DOI: 10.1039/C4NJ02427C

gene bank: Bcl-2 (F), 5`-TGCACCTGACGCCCTTCAC-3`; Bcl-2 (R), 5`-AGACAGCCAGGAGAAATCAAACAG-3`. Bax (F), 5`-ACCAAGAAGCTGAGCGAGTGTC-3`; Bax (R), 5`-ACAAAGATGGTCACGGTCTGCC-3`. $p21^{WAF-1}$ (F), 5`-GGGGAC-AGCAGAGGAAGAC-3`; p21WAF1 (R), 5`-CGGCGTTTGGAGTGGTAGA-3`. GAPDH (F), 5`-ACCCAGAAGACTGTGGATGG-3`; GAPDH (R), 5`-CCCCTCTTCAAGGGGTCTAC-3`. The PCR products were separated using 1.5% agarose gels. After the gels were stained with ethidium bromide, gel images were obtained and the densities of the products were quantified using Gel-Pro Analyzer 4.0 Software (Media Cybernetics, USA). All experiments were repeated at least four times.

4.7.4. Statistical Analysis: Data were compared by one-way analysis of variance Student's t-test to determine statistical significance (Sigmaplot©11). Each experiment is performed in triplicate on 4 occasions. Results are expressed as mean ± SD. Differences with P values of < 0.05 were considered significant.

4.8 Computational Details

The Gaussian 03 computational package[49] was used to perform ground-state and transition-state geometry optimization calculations employing Becke's three-parameter hybrid exchange functional and the Lee–Yang–Parr nonlocal correlation functional B3LYP[50-52] and the 6-31G* basis set was used for S, C, N, O, and H atoms[53]. Time-dependent density functional theory calculations were also performed using this methodology, and the first 60 singlet excited states were calculated. Calculations by the first-principles method were used to obtain accurate excitation energies and oscillator strengths. We modelled the solvent with the polarizable continuum model using ethanol as the solvent[54].

View Article Online
DOI: 10.1039/C4NJ02427C

Acknowledgements: The authors acknowledge the financial support received from the Fondo Nacional de Ciencia y Tecnología of Chile, (FONDECYT, Grants No. 1080269, 1090341, 1120514, 1130707), Ministerio de Economía y Competitividad of Spain (Grants CTQ2009-12520-C03-03, FEDER funds and CONSOLIDER CSD2007-41) and Pla de Recerca de Catalunya (Grants 2009SGR-203).

Supplementary Information

(The CCDC reference numbers for compounds (**7**) and (**17**) are 882688 and 882689, respectively)

References

1. For a brief review see: Carlsen, L.; Döpp, D.; Döpp, H.; Duus, F.; Hartmannn, H; Lang-Fugmann, S; Schulze, B; Smalley, R. K.; Wakefield, B. J. In *Houbent-Weyl, Methods in Organic Chemistry*; Schaumann, E.; Ed., Georg Thieme Verlag: Stuttgard Germany, **1992**; Vol. E8a, pp 45-204.
2. Rowley, M.; Broughton, H. B.; Collins, I.; Baker, R.; Emms, F.; Marwood, R.; Patel, S.; Ragan, C. I.; Freedman, S. B.; Leeson, P. D. *Journal of Medicinal Chemistry* **1996,** *39*, 1943.
3. Frolund, B.; Jorgensen, A. T.; Tagmose, L.; Stensbol, T. B.; Vestergaard, H. T.; Engblom, C.; Kristiansen, U.; Sanchez, C.; Krogsgaard-Larsen, P.; Liljefors, T. *Journal of Medicinal Chemistry* **2002,** *45*, 2454.
4. Daidone, G.; Raffa, D.; Maggio, B.; Plescia, F.; Cutuli, V. M. C.; Mangano, N. G.; Caruso, A. *Archiv Der Pharmazie* **1999,** *332*, 50.

View Article Online
DOI: 10.1039/C4NJ02427C

5. Bhatt, A. H.; Parekh, H. H.; Parikh, A. R. *Heterocyclic Communications* **1998,** *4*, 361.

6. Talley, J. J.; Bertenshaw, S. R.; Brown, D. L.; Carter, J. S.; Graneto, M. J.; Kellogg, M. S.; Koboldt, C. M.; Yuan, J. H.; Zhang, Y. Y.; Seibert, K. *Journal of Medicinal Chemistry* **2000,** *43*, 1661.

7. Talley, J. J.; Brown, D. L.; Carter, J. S.; Graneto, M. J.; Koboldt, C. M.; Masferrer, J. L.; Perkins, W. E.; Rogers, R. S.; Shaffer, A. F.; Zhang, Y. Y.; Zweifel, B. S.; Seibert, K. *Journal of Medicinal Chemistry* **2000,** *43*, 775.

8. Giovannoni, M. P.; Vergelli, C.; Ghelardini, C.; Galeotti, N.; Bartolini, A.; Dal Piaz, V. *Journal of Medicinal Chemistry* **2003,** *46*, 1055.

9. Li, W. T.; Hwang, D. R.; Chen, C. P.; Shen, C. W.; Huang, C. L.; Chen, T. W.; Lin, C. H.; Chang, Y. L.; Chang, Y. Y.; Lo, Y. K.; Tseng, H. Y.; Lin, C. C.; Song, J. S.; Chen, H. C.; Chen, S. J.; Wu, S. H.; Chen, C. T. *Journal of Medicinal Chemistry* **2003,** *46*, 1706.

10. See Wakefield, B. J. In *Science of Synthesis: Houbent-Weyl Methods of Molecular transformations*; Shaumann, E., Ed.; Georg Thieme Verlag: Stuttgart **2001**; Vol. 11, 229-288.

11. Bandiera, T.; Grunanger, P.; Albini, F. M. *Journal of Heterocyclic Chemistry* **1992,** *29*, 1423.

12. Cuadrado, P.; Gonzalez-Nogal, A. M.; Valero, R. *Tetrahedron* **2002,** *58*, 4975.

13. Vicentini, C. B.; Veronese, A. C.; Poli, T.; Guarneri, M.; Giori, P.; Ferretti, V. *Journal of Heterocyclic Chemistry* **1990,** *27*, 1481.

14. He, Y.; Lin, N. H. *Synthesis-Stuttgart* **1994**, 989.

15. Barber, G. N.; Olofson, R. A. *Journal of Organic Chemistry* **1978,** *43*, 3015.

16. Nitz, T. J.; Volkots, D. L.; Aldous, D. J.; Oglesby, R. C. *Journal of Organic Chemistry* **1994,** *59*, 5828.

17. Denmark, S. E.; Kallemeyn, J. M. *Journal of Organic Chemistry* **2005**, *70*, 2839.

View Article Online
DOI: 10.1039/C4NJ02427C

18. See Jaerger, V.; Colinas, P. A. In *Synthetic Applications of 1,3-Dipolar Cicloaddition Chemistry Toward Heterocycles and Natural Products*; Padwa, A., Pearson, W. H., Eds.; Chemistry of Heterocyclic Compounds; Wiley; Hoboken, **2002**; Vol. 59, pp 361-472.

19. Day, R. A.; Blake, J. A.; Stephens, C. E. *Synthesis-Stuttgart* **2003**, 1586.

20. Burkhard, J. A.; Tchitchanov, B. H.; Carreira, E. M. *Angewandte Chemie-International Edition* 2011,*50*, 5379.

21. Ueda, M.; Sato, A.; Ikeda, Y.; Miyoshi, T.; Naito, T.; Miyata, O. *Organic Letters* **2010**, *12*, 2594. ; Masafumi Ueda , Shoichi Sugita , Aoi Sato , Tetsuya Miyoshi , and Okiko Miyata, J. Org. Chem., **2012**, *77* (20), 9344

22. Ueda, M.; Ikeda, Y.; Sato, A.; Ito, Y.; Kakiuchi, M.; Shono, H.; Miyoshi, T.; Naito, T.; Miyata, O. *Tetrahedron* **2011**, *67*, 4612.

23. Alvarez-Thon, L.; Bustos, C.; Schott, E.; Sanchez, C.; Ibanez, A. *Acta Crystallogr. Sect. E.-Struct Rep. Online* **2006**, *62*, O595.

24. Yao, H. C. *Journal of Organic Chemistry* **1964**, 29, 2959-2963.

25. Marten, J.; Seichter, W.; Weber, E.; Boehme, U. *Journal of Physical Organic Chemistry* **2007**, *20*, 716.

26. Bertolasi, V.; Gilli, P.; Ferretti, V.; Gilli, G.; Vaughan, K. *New Journal of Chemistry* **1999**, *23*, 1261.

27. Bustos, C.; Sanchez, C.; Martinez, R.; Ugarte, R.; Schott, E.; Carey, D. M. L.; Garland, M. T.; Espinoza, L. *Dyes and Pigments* **2007**, *74*, 615.

28. Bey, E.; Marchais-Oberwinkler, S.; Kruchten, P.; Frotscher, M.; Werth, R.; Oster, A.; Algul, O.; Neugebauer, A.; Hartmann, R. W. *Bioorganic & Medicinal Chemistry* **2008,** *16*, 6423.

29. Garattini, E.; Parrella, E.; Diomede, L.; Gianni, M.; Kalac, Y.; Merlini, L.; Simoni, D.; Zanier, R.; Ferrara, F. F.; Chiarucci, I.; Carminati, P.; Terao, M.; Pisano, C. *Blood* **2004,** *103*, 194.

View Article Online
DOI: 10.1039/C4NJ02427C

30. Kaffy, J.; Pontikis, R.; Carrez, D.; Croisy, A.; Monneret, C.; Florent, J. C. *Bioorganic & Medicinal Chemistry* **2006,** *14*, 4067.

31. Simoni, D.; Rondanin, R.; Baruchello, R.; Rizzi, M.; Grisolia, G.; Eleopra, M.; Grimaudo, S.; Di Cristina, A.; Pipitone, M. R.; Bongiorno, M. R.; Arico, M.; Invidiata, F. P.; Tolomeo, M. *Journal of Medicinal Chemistry* **2008,** *51*, 4796.

32. Sun, C. M.; Lin, L. G.; Yu, H. J.; Cheng, C. Y.; Tsai, Y. C.; Chu, C. W.; Din, Y. H.; Chau, Y. P.; Don, M. J. *Bioorganic & Medicinal Chemistry Letters* **2007,** *17*, 1078.

33. Fisher, D. E. *Cell* **1994,** *78*, 539.

34. Sherr, C. J. *Cell* **1993,** *73*, 1059.

35. Hunter, T. *Cell* **1993,** *75*, 839.

36. Kato, J.; Matsushime, H.; Hiebert, S. W.; Ewen, M. E.; Sherr, C. J. *Genes & Development*, **1993,** *7*, 331.

37. Eldeiry, W. S.; Tokino, T.; Velculescu, V. E.; Levy, D. B.; Parsons, R.; Trent, J. M.; Lin, D.; Mercer, W. E.; Kinzler, K. W.; Vogelstein, B. *Cell* **1993,** *75*, 817.

38. Xiong, Y.; Hannon, G. J.; Zhang, H.; Casso, D.; Kobayashi, R.; Beach, D. *Nature* **1993,** *366*, 701.

39. Desiraju, G.R.; Sarma, J.A.R.P. *Proceedings of the Indian Academy of Sciences-Chemical Sciences* **1986**, *96*, 599.

40. Farrugia, L. J.; *Journal of Applied. Crystallography* **1999**, *32*, 837.

41. Burla, M.C.; Caliandro, R.; Camalli, M.; Carrozzini, B.; Cascarano, G. L.; De Caro, L.; Giacovazzo, C; Polidori, G.; Spagna; R. *Journal of Applied. Crystallography* **2005,** *38*, 381.

42. Sheldrick, G.M. SHELXL97. *Program for Crystal Structure Analysis* (Release 97-2), University of Göttingen, Göttingen, Germany, **1997**.

43. Pauling L. *The Journal of American Chemistry Society* **1947,** *69,* 542.

View Article Online
DOI: 10.1039/C4NJ02427C

44. Freshney, R. I. Culture of Animal Cells. *A manual of basic techniques*. Alan Liss Inc. (University Library) **1983**, 17.

45. Paul, J. *Cell and Tissue Culture*. *Churchill Livingstone* (CSL) **1975**.

46. Mosmann, T. *Journal of Immunolical Methods*, **1983**, *65,* 55.

47. Tchounwou, P. B.; Wilson, B.; Schneider, J.; Ishaque, A. *Metal Ions Biology and Medicine* **2000**, *6*, 89.

48. Chomczynski P, Sacchi N. *Analytical Biochemistry* **1987**, *162*, 156.

49. Gaussian 03, Revision C.02, M. J. Frisch, G. W. Trucks, H. B. Schlegel, G. E. Scuseria, M. A. Robb, J. R. Cheeseman, J. A. Montgomery, Jr., T. Vreven, K. N. Kudin, J. C. Burant, J. M. Millam, S. S. Iyengar, J. Tomasi, V. Barone, B. Mennucci, M. Cossi, G. Scalmani, N. Rega, G. A. Petersson, H. Nakatsuji, M. Hada, M. Ehara, K. Toyota, R. Fukuda, J. Hasegawa, M. Ishida, T. Nakajima, Y. Honda, O. Kitao, H. Nakai, M. Klene, X. Li, J. E. Knox, H. P. Hratchian, J. B. Cross, V. Bakken, C. Adamo, J. Jaramillo, R. Gomperts, R. E. Stratmann, O. Yazyev, A. J. Austin, R. Cammi, C. Pomelli, J. W. Ochterski, P. Y. Ayala, K. Morokuma, G. A. Voth, P. Salvador, J. J. Dannenberg, V. G. Zakrzewski, S. Dapprich, A. D. Daniels, M. C. Strain, O. Farkas, D. K. Malick, A. D. Rabuck, K. Raghavachari, J. B. Foresman, J. V. Ortiz, Q. Cui, A. G. Baboul, S. Clifford, J. Cioslowski, B. B. Stefanov, G. Liu, A. Liashenko, P. Piskorz, I. Komaromi, R. L. Martin, D. J. Fox, T. Keith, M. A. Al-Laham, C. Y. Peng, A. Nanayakkara, M. Challacombe, P. M. W. Gill, B. Johnson, W. Chen, M. W. Wong, C. Gonzalez, and J. A. Pople, Gaussian, Inc., Wallingford CT, 2004

50. A.D. Becke, *Phys. Rev. A* **1988**, 38, 3098.

51. C. Lee; W. Yang, R.G. Parr, *Phys. Rev. B* **1988**, 37, 785.

52. A.D. Becke, *J. Chem. Phys.* **1993**, 98, 5648.

53. P.J. Hay; W.R. Wadt, *J. Chem. Phys.* **1985**, 82, 270.

54. M. Cossi; G. Scalmani; N. Rega, V. Barone, *J. Chem. Phys.* **2002**, 117, 43.